1   *Title:* Glucose limitation in *Lactococcus* shapes a single-peaked fitness landscape exposing

2   membrane occupancy as a constraint

3

4   *Authors:*

5   Claire E. Price[a,b,c,1,2], Filipe Branco dos Santos[c,d,e,2], Anne Hesseling[a], Jaakko J. Uusitalo[f],

6   Herwig Bachmann[c,d], Vera Benavente[d], Anisha Goel[c,d], Jan Berkhout[d], Frank J. Bruggeman[d],

7   Siewert-Jan Marrink[f], Manolo Montalban-Lopez[a], Anne de Jong[a], Jan Kok[a], Douwe

8   Molenaar[c,d], Bert Poolman[b], Bas Teusink[c,d], Oscar P. Kuipers[a,c]

9

10   *Author affiliations:*

11   [a] Molecular Genetics group, University of Groningen, Nijenborgh 7, 9747 AG Groningen, the

12   Netherlands

13   [b] Department of Biochemistry, University of Groningen, Nijenborgh 4, 9747 AG Groningen,

14   the Netherlands

15   [c] Kluyver Center for Genomics of Industrial Fermentations/NCSB, Julianalaan 67, 2628 BC

16   Delft, The Netherlands

17   [d] Systems Bioinformatics, Faculty of Earth and Life Sciences, VU University Amsterdam, De

18   Boelelaan 1085, 1081 HV Amsterdam, The Netherlands

19   [e] Molecular Microbial Physiology Group, Faculty of Life Sciences, Swammerdam Institute of

20   Life Sciences, University of Amsterdam, Science Park 904, Amsterdam 1098 XH,

21   Netherlands

22   [f] Molecular Dynamics group, University of Groningen, Nijenborgh 7, 9747 AG Groningen,

23   the Netherlands

24

25   *Author footnotes:*

26   [1] Current address: DSM Biotechnology Centre, Alexander Fleminglaan 1, 2613 AX, Delft,

27   the Netherlands

28   [2] Both authors contributed equally

29   [3] Current address: Chr. Hansen, Boege Allé 10-12, 2970 Hoersholm, Denmark

30

31

32   *Corresponding authors:* b.teusink@vu.nl and o.p.kuipers@rug.nl

33

34   *Keywords:* evolution, systems biology, lactic acid bacteria, resource allocation

35

36   **ABSTRACT**

37   A central theme in biology is to understand the molecular basis of fitness: which strategies

38   succeed under which conditions; how are they mechanistically implemented; and which

39   constraints shape trade-offs between alternative strategies. We approached these questions

40   with parallel bacterial evolution experiments in chemostats. Chemostats provide a constant

41   environment with a defined resource limitation (glucose), in which the growth rate can be

42   controlled. Using *Lactococcus lactis*, we found a single mutation in a global regulator of

43   carbon metabolism, CcpA, to confer predictable fitness improvements across multiple growth

44   rates. *In silico* protein structural analysis complemented with biochemical and phenotypic

45   assays, show that the mutation reprograms the CcpA regulon, specifically targeting

46   transporters. This supports that membrane occupancy, rather than biosynthetic capacity, is the

47   dominant constraint for the observed fitness enhancement. It also demonstrates that cells can

48   modulate a pleiotropic regulator to work around limiting constraints.

49

50   **INTRODUCTION**

51   Many microorganisms have a remarkable versatility to adapt to different environments, either

52   at the short time scale through signaling and gene expression networks, or at an evolutionary

53   time scale through genomic adaptations to selective pressures. A key question in

54   (micro)biology, is how specific selective pressures shape molecular strategies, how evolvable

55   they are, and which constraints and resulting trade-offs in phenotypic traits are relevant under

56   what condition.

57   In recent years a number of studies (Dekel and Alon, 2005; Molenaar *et al.*, 2009; Scott *et al.*,

58   2010, 2014) pointed towards cellular resource limitations, born from environmental

59   (nutritional) constraints but also from intrinsic kinetic and physicochemical constraints, as

60   main forces for regulatory strategies. These relate to the role of protein costs in particular,

61   and how the need for ribosomal protein synthesis capacity requires growth-rate dependent

62   regulation of the proteome (Scott *et al.*, 2010). Although these concepts can explain many

63   regulatory phenomena, such as catabolite repression (Görke and Stülke, 2008) and overflow

64   metabolism (Basan *et al.*, 2015), it remains to be demonstrated (i) to what extent such

65   strategies require optimality or are optimal solutions to the resource allocation problem; (ii)

66   what exactly the constraints are that govern the resource allocation; (iii) what the regulatory

67   mechanisms are that result in proteome re-allocation; and (iv) whether these concepts apply

68   to microorganisms other than *E. coli* – the organism for which these concepts have been

69   largely developed and experimentally tested.

70   We have recently challenged the view that protein costs play a role in metabolic switches in

71   the lactic acid bacterium *Lactococcus lactis*: we found a switch from mixed acid fermentation

72   to homolactic fermentation (an anaerobic variant of the Crabtree effect) in the absence of

73   proteome alterations (Goel, Eckhardt, Puri, Jong, Branco dos Santos, Giera, Fusetti, Vos,

74   Kok, Poolman, Molenaar, Kuipers and Teusink, 2015). One explanation was that this

75   bacterium might not display optimal behaviour in the chemostat in which they were

76   cultivated. This primed us to do laboratory evolution experiments as they offer unique

77   opportunities for the testing of adaptive strategies, whilst monitoring evolving populations

78   under well-defined conditions.

79   Laboratory evolution of microorganisms can be carried out under a broad range of selective

80   pressures, such as varying growth rate in serial batch cultures (Bachmann *et al.*, 2012; Wiser,

81   Ribeck and Lenski, 2013), antibiotic resistance in different cultivation settings (Lázár *et al.*,

82   2013), growth rate under nutrient limitation in chemostats (Gresham and Hong, 2014), cell

83   number in emulsion-based systems (Bachmann *et al.*, 2013), and growth rate in dynamic

84   environments (Meadows *et al.*, 2010). However, to study the role of limited resource

85   allocation on adaptive strategies, at different growth rates and evolutionary time scales, the

86   chemostat is perfect (Gresham and Hong, 2014). It allows for full control over the nature of

87   the resource limitation and the growth rate, and provide a constant, steady-state environment.

88   We studied microbial evolution of *Lactococcus lactis* in highly-standardized glucose-limited

89   chemostats at two different dilution rates with four replicates each. We found the exact same

90   residue of a pleiotropic regulator to be mutated in all of these experiments, and confirm the

91   fitness-enhancing effect of this mutation in chemostat competition experiments at other

92   dilution rates as well. Detailed characterization of the biochemical and phenotypical

93   consequences of the mutation demonstrated a reprogramming of the regulatory logic of the

94   regulator, by inducing the suppression of alternative carbon uptake systems under low

95   glucose levels whilst maintaining the –otherwise similarly regulated- high affinity glucose

96   transporter. The occurrence of one dominant mutation suggests a single-peaked fitness

97   landscape and shows that the dominant constraint under such chemostat conditions is not

98   cytosolic protein synthesis costs, but rather membrane occupancy. We thus experimentally

99   confirm and extend previous computational studies in *E coli* (O'Brien *et al.*, 2013) which

100   suggested the action of different constraints (nutrient limitation and proteome limitation)

101   under different conditions. While doing so, we provide a full mechanistic mapping from

102   mutation to regulation to fitness.

103

104   **RESULTS**

105   *Chemostat and cultivation design for long-term microbial evolution under stable*

106   *environmental conditions*

107   Until now, microbial evolution in chemostats has been rather limited by the number of

108   replicates and by the number of generations, *i.e.* volume changes. Initially described as a

109   device that could continuously cultivate bacteria for an indefinite period of time (Novick and

110   Szilard, 1950), to date the longest published cultivation using a chemostat is only a few

111   hundred generations (Gresham and Hong, 2014). This is several orders of magnitude shorter

112   than the longest serial batch cultivation experiments – 50,000 generations and counting

113   (Wiser, Ribeck and Lenski, 2013). To address the failure of long-term continuous cultivation,

114   we developed a versatile bioreactor cap and experimental set-up to perform parallel,

115   prolonged cultivations under chemostat conditions, at small working volumes (detailed in

116   Supplementary Materials and Figure 1). These advances allowed us to conduct experiments

117   in quadruplicate for more than 1000 consecutive generations.
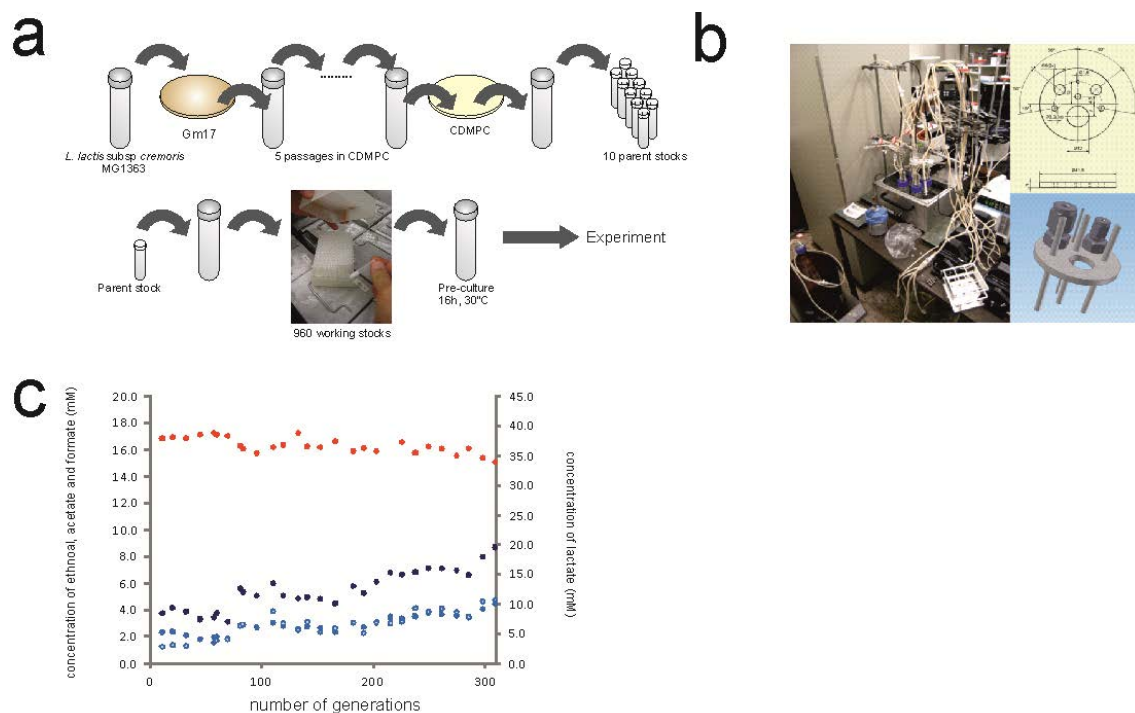
118

119

120   **Figure 1.** (a) Standardized cryopreservation procedure to minimize strain variability among
121   experiments. GM17: M17 medium supplemented with 25 mM glucose, CDMPC: chemically
122   defined medium for prolonged cultivation. (b) Miniaturized chemostat set up to allow
123   prolonged cultivation experiments in parallel and (c) the online measurements of organic
124   acids for strain 309C1 taken during the evolution experiments at D of 0.5 h-1 showing lactate
125   (red), formate (dark blue), acetone (blue) and ethanol (light blue).

126

127

128   Additionally, a requirement of laboratory evolution is that sources of technical variability

129   between replicates are minimized. Our initial focus was set on carefully defining the

130   cultivation conditions (chemostat and medium) and on standardizing experimental procedures

131   (inoculation, sampling, and cell storage). We developed a chemically defined medium

132   particularly suited for prolonged cultivation (CDMPC) based on the nutrient requirements

133   (Jensen and Hammer, 1993) and biomass composition of *L. lactis* MG1363 (Oliveira, Nielsen

134   and Förster, 2005) (detailed in supplementary materials). To reduce inoculum variability we

135   implemented a strictly controlled cryopreservation and inoculation procedure (Figure 1 and

136   detailed in Supplementary Materials).

137   The cultivation history of bacterial strains is of upmost importance. Strains can rapidly

138   deviate from their original genotype, which can lead to noticeable phenotypic differences

139   (Linares, Kok and Poolman, 2010; Bachmann *et al.*, 2012). Our initial inoculum came from

140   the original *L. lactis* MG1363 sequenced stock (Linares, Kok and Poolman, 2010). Since our

141   newly designed medium could potentially lead to the selection of new genotypes, we

142   performed a short-term serial batch adaptation of this strain to the medium CDMPC. The

143   resulting single isolate picked (Genr0) was cryopreserved and used as the seeding population

144   for all the laboratory evolution experiments performed.

145   *Parallel laboratory evolution in chemostat cultures*

146   We exposed *L. lactis* MG1363 to parallel chemostat cultivations: Genr0 was cultivated

147   continuously in quadruplicate, each using 60 mL glucose-limited chemostats at a growth rate

148   of $0.5h^{-1}$ for over 300 volume changes. Culture samples were harvested periodically every

149   10-15 generations from the effluent to determine cell density and the fluxes of fermentation

150   substrates and products (an example is given in Figure 1C). Cell samples were stored as

151   glycerol stocks at -80°C to be used as snapshots of the evolutionary process.

6

152   Throughout the prolonged cultivation, all four replicates (referred hereon as 309C1 through

153   309C4) displayed very similar behavior. Biomass concentration did not vary significantly

154   indicating that biomass yield on substrate remained fairly constant (Supplementary Figure 1).

155   *L. lactis* can catabolize glucose through homolactic or mixed acid fermentation, excreting,

156   respectively, lactate, or acetate, formate and ethanol (Thomas, Ellwood and Longyear, 1979).

157   At a dilution rate of 0.5 h^{-1}, Genr0 produces mainly lactate (lactate:acetate ratio ~16).

158   Throughout the course of the experiment, all parallel reactors shifted gradually towards

159   mixed acid fermentation leading to a ratio of approximately 7. Despite the fact that this

160   fermentative mode leads to a theoretical 50% increase in ATP yield, the biomass

161   concentration did not change. The latter can be explained by the observation that the evolved

162   cells also gradually excreted more pyruvate, the final shared precursor of the homolactic and

163   the mixed acid fermentative pathways (Supplementary Figure 1).

164   When evolved cells were grown on glucose in batch, we observed differences with Genr0 in

165   the maximal growth rate (μ_{max}), length of the lag phase and sedimentation. We compared to

166   Genr0 both the population samples collected after 309 generations and single colony isolates

167   from the evolved population samples (Supplementary Figures 1 and 6). Irrespective of

168   whether the evolved populations or the isolates were compared, they were clearly

169   outperformed by Genr0 in batch. Most notably, μ_{max} dropped to a value close to the dilution

170   rate at which cells were evolved, which falls nearly 25% below the μ_{max} of the parent strain.

171   The evolved strains also exhibited extended lag phases and sedimentation during batch

172   cultivations. The sedimentation was reminiscent of the AcmA-deficient phenotype previously

173   described (Buist *et al.*, 1995).

174   *Identification of the mutations arising during the evolutionary experiment*

175   We sequenced single-colony isolates from the original strain stock of Genr0 and from the end

176   of the four replicate evolution experiments performed at a dilution rate of 0.5h^{-1} (*i.e.* 309C1,

7

177   309C2, 309C3, 309C4). The published whole genome sequence for *L. lactis* MG1363

178   (Linares, Kok and Poolman, 2010) was used as a reference for sequence assembly. Mutations

179   were identified and verified by Sanger sequencing (Supplementary Table 2). In comparison

180   with Genr0, we found SNPs unique to the evolved strains (Figure 2). The number of SNPs

181   accumulated per genome was between one (309C1) and six (309C4). This corresponds to a

182   mutation rate of 1.3 to 7.8 x 10^{-9} (per base pair per generation) and is in line with currently

183   published estimates (Barrick *et al.*, 2009).

184

185
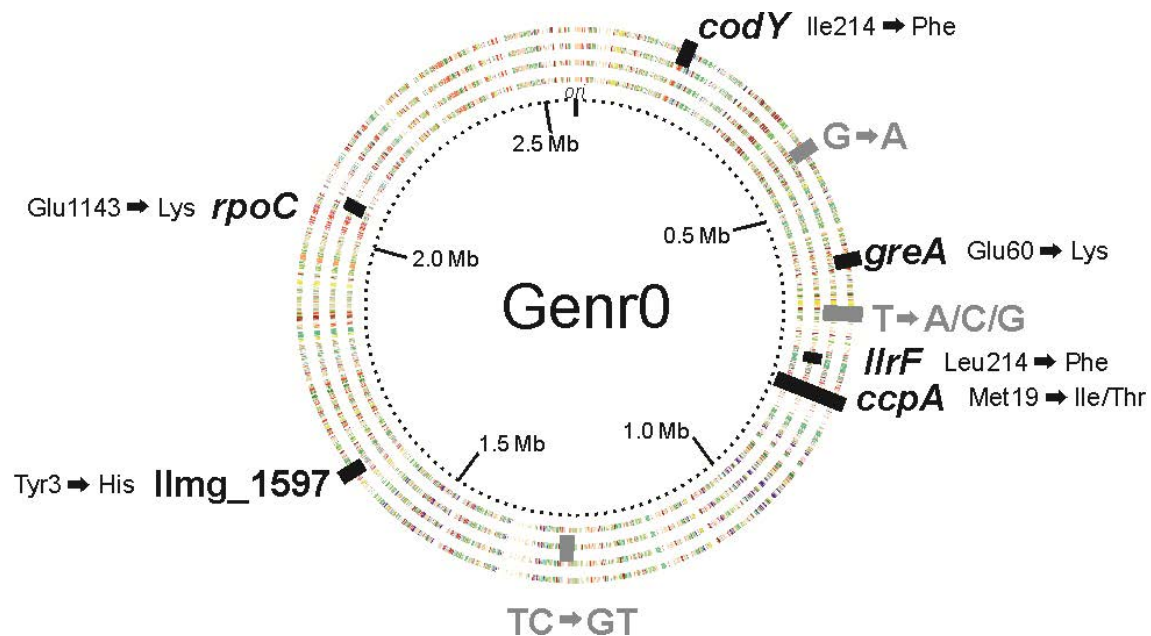
186   **Figure 2. Mutations identified in the 4 evolved strains compared to the original strain**
187   **Genr0.** The genes and intergenic regions with SNP mutations are shown. For coding regions
188   (in black) the resulting amino acid substitution is indicated. The dotted inner ring indicates
189   the genome position. The rings are color-coded according to the COG-classification of the
190   gene present on the forward and reverse strands, and from inner to outer ring we represent
191   evolved strains 309C1 to C4.

192

193

8

194   All of the SNPs in the coding regions were non-synonymous (more details in Supplementary

195   Materials), and strikingly, all strains accumulated a mutation in the codon coding for Met19

196   in the global transcriptional regulator CcpA of Genr0. At the DNA level, the mutations

197   differed between the evolved strains. In strains 309C1, 309C2, and 309C3, ATG was mutated

198   to either ATA or ATC, resulting in the amino acid change from Met to Ile. In none of the

199   sequencing experiments performed for cells cultured at a D of $0.5h^{-1}$ was the Ile codon ATT

200   identified (see also section on *Dynamics of Evolution Experiments*). For strain 309C4 the

201   ATG codon was mutated to ACG resulting in a Met to Thr change. Strains 309C2, 309C3 and

202   309C4 contain a few additional mutations, while the isolate of 309C1 only contains the SNP

203   in *ccpA*. Since 309C1 exhibits very similar phenotypes to those of the other strains, this

204   mutation must be sufficient to confer a growth advantage to the evolved strains when

205   compared to Genr0, and to a great extent be the genetic basis of the common phenotypic

206   differences observed. These include the growth kinetics and sedimentation phenotype

207   (Supplementary Figures 1 and 6) and, as addressed below, altered glucose utilization kinetics.

208   The sequences were also analyzed for insertions and/or deletions and when compared to the

209   Genr0 sequence; the evolved strains showed no major frameshifts (see Supplementary Table
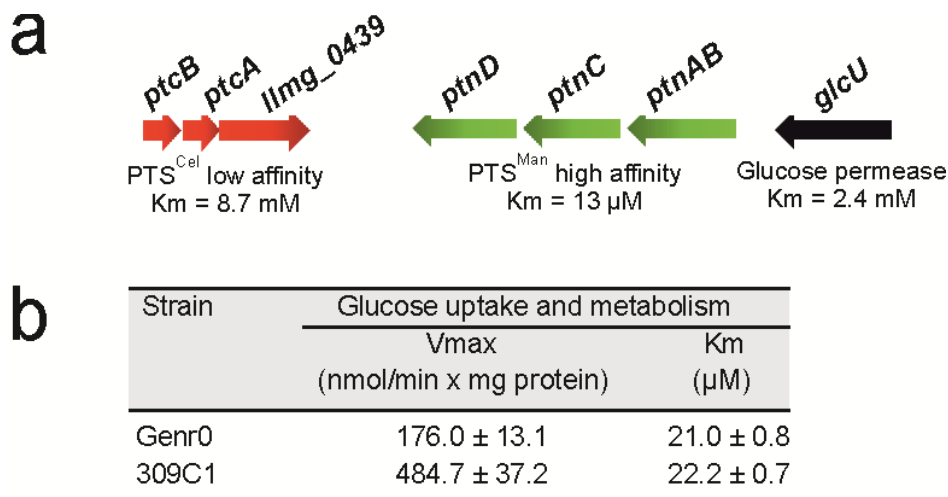
210   2).

211   *Effect of CcpA M19I on global gene expression patterns*

212   The evolved strains were revived in CDMPC and grown until mid-exponential phase at

213   which point microarray analyses were performed (Kuipers *et al.*, 2002). Gene expression in

214   the evolved strains was compared to that of Genr0. Evolved strain 309C1, which contains

215   only the SNP in *ccpA,* showed an altered gene expression dominated by genes involved in

216   membrane transport, especially carbohydrate import (Supplementary Figure 3,

217   Supplementary Table 3, Supplementary Table 4). CcpA controls the preferential use of

218   glucose over other sugars (Deutscher, Francke and Postma, 2006) and regulon analysis of the

219   differentially expressed genes revealed that CcpA-regulated genes were indeed over-

220   represented in the data set.

221   *L. lactis* contains three glucose import systems – two phosphotransferase systems, PTS^{Man}

222   and PTS^{Cel}, and a glucose facilitated diffusion system (Castro *et al.*, 2009) – and expression

223   of the genes encoding the high affinity PTS^{Man} were up-regulated compared to the original

224   strain, while those encoding the low affinity PTS^{Cel} were down-regulated (Figure 3A). The

225   effects of these gene expression changes were investigated further by monitoring the uptake

226   of ^{14}C-glucose in whole cells. In accordance with the sequencing and gene expression data,

227   *i.e.* the glucose transporters themselves are not mutated but rather their expression is

228   changed: the rate at which glucose was taken up by the cells was increased nearly 3-fold in

229   the evolved strain, while the apparent Michaelis constant for glucose was unchanged (Figure

230   3B).

231

Strain	Glucose uptake and metabolism	
	Vmax (nmol/min x mg protein)	Km (µM)
Genr0	176.0 ± 13.1	21.0 ± 0.8
309C1	484.7 ± 37.2	22.2 ± 0.7

232

233   **Figure 3. Altered gene expression in strain 309C1 is focused on transport pathways.** (a)
234   The expression of genes involved in glucose uptake in *L. lactis* MG1363 was significantly
235   changed in the evolved strains. Highlighted in green are genes that were up-regulated and in
236   red those that were down-regulated. (b) Kinetic parameters of glucose transport in Genr0 and
237   strain 309C1 were determined in cells grown to exponential phase in CDMPC. Glucose
238   transport was assayed with [^{14}-C]-labeled glucose. Values of three independent experiments
239   were averaged and are reported ±SD. V_{max} and K_m were determined using glucose
240   concentrations from 1.2 to 200 µM (Gouridis *et al.*, 2015).
241

242   The ability to utilize other carbon sources was diminished for the evolved strains

243   (Supplementary Figure 4A). This coincided with the down regulation of, amongst others,

244   genes encoding for maltose transporters, ABC sugar importers and sugar utilization enzymes

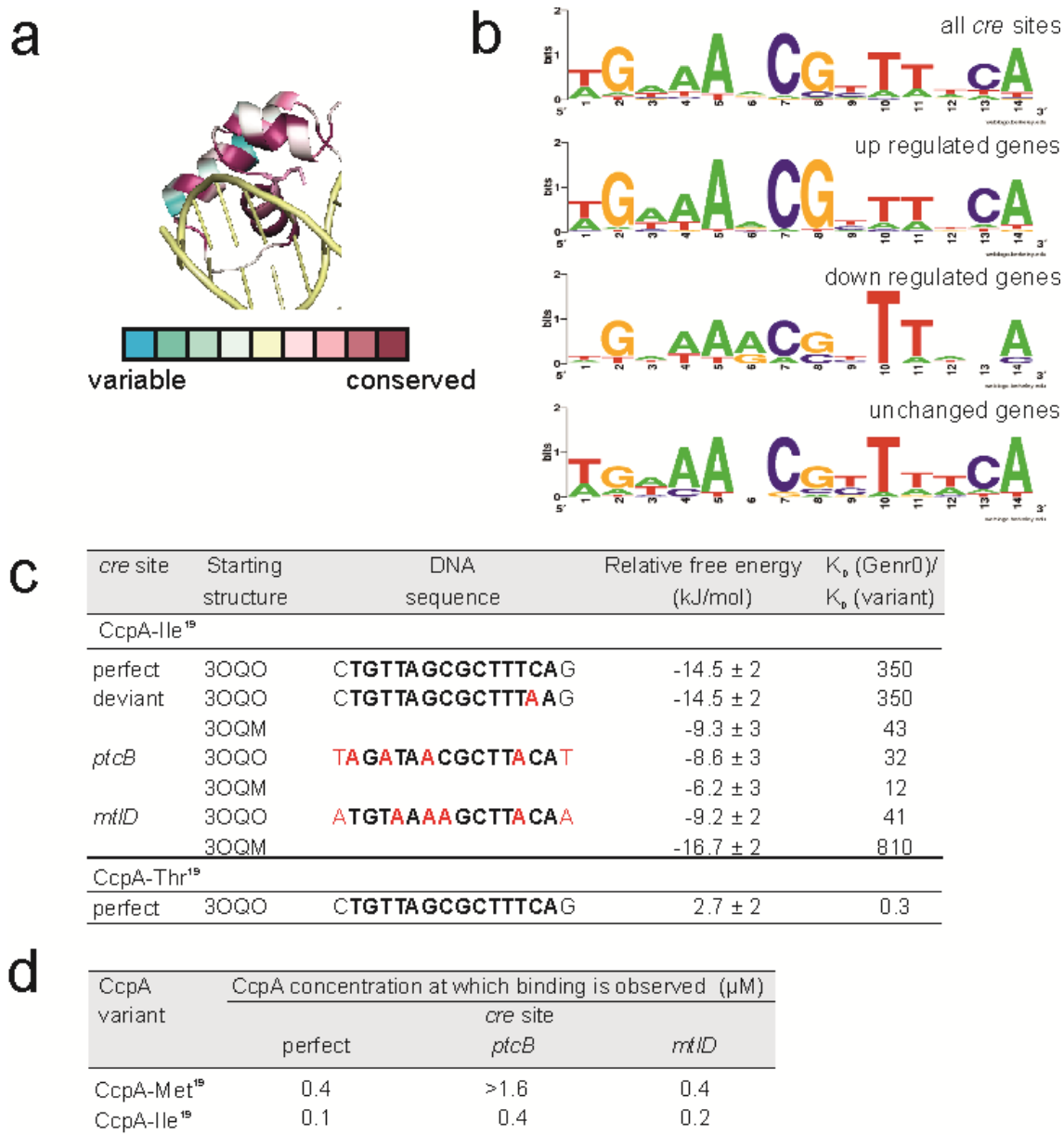245   (Supplementary Table 3), many of which are CcpA-regulated.

246   In general, CcpA is a versatile global regulator that can act as a transcriptional repressor or

247   activator. An amino acid substitution in the DNA binding region may therefore have

248   qualitatively different effects at different target promoters. This is indeed what we observe:

249   15 CcpA-regulated genes are down regulated, 6 are up-regulated, while 11 remain

250   unchanged. We next examined the molecular basis of the differential effects on expression.

251   *Effect of M19I mutation on the binding affinity of CcpA*

252   Met19 is located in the second helix of the DNA-binding domain and is highly conserved in

253   CcpA (Figure 4A and Supplementary Figure 8). *L. lactis* CcpA binds to *cre* sites for which

254   the consensus sequence is known: TGNNANCGNTTNCA. Sequence analysis revealed that

255   putative *cre* sites upstream down-regulated genes were closest to the *cre* consensus sequence,

256   while up-regulated genes deviated and were less likely to have both C7, G8 and C13 but

257   always T10 (Figure 4B). We tested this further by analyzing CcpA with either Met or Ile or

258   Thr at position 19 and a select number of *cre* site sequences in *in vitro* binding assays and

259   molecular dynamic simulations.

260   For all 4 *cre* sites tested *in vitro*, the CcpA-Ile19 variant showed an increase in binding

261   affinity for the DNA operators selected (Figure 4D and Supplementary Figure 10). This was

262   most pronounced for the sequence upstream of *ptcB* and least pronounced for *mtlD*. To

263   complement the binding assays, molecular dynamic simulations were performed. This

264   allowed us to determine the relative binding free energy of the CcpA variants to a similar set

265   of DNA operators (Figure 4C, Supplementary Figure 9).

266

a

b

all cre sites

up regulated genes

down regulated genes

unchanged genes

variable   conserved

c

cre site	Starting structure	DNA sequence	Relative free energy (kJ/mol)	K_D (Genr0)/ K_D (variant)
CcpA-Ile[19]				
perfect	3OQO	CTGTTAGCGCTTTCAG	-14.5 ± 2	350
deviant	3OQO	CTGTTAGCGCTTTAAG	-14.5 ± 2	350
	3OQM		-9.3 ± 3	43
ptcB	3OQO	TAGATAACGCTTACAT	-8.6 ± 3	32
	3OQM		-6.2 ± 3	12
mtlD	3OQO	ATGTAAAAGCTTACAA	-9.2 ± 2	41
	3OQM		-16.7 ± 2	810
CcpA-Thr[19]				
perfect	3OQO	CTGTTAGCGCTTTCAG	2.7 ± 2	0.3

d

CcpA variant	CcpA concentration at which binding is observed (µM)		
	cre site		
	perfect	ptcB	mtlD
CcpA-Met[19]	0.4	>1.6	0.4
CcpA-Ile[19]	0.1	0.4	0.2

Figure 4. Mutations in *ccpA* result in increased binding affinity for certain *cre* sites. Mutations in the Met[19] codon in the DNA binding domain of CcpA alter the binding affinity of CcpA for certain *cre* sites. (a) View of the DNA-binding domain with the side chain of Met19. Using ConSurf 2010 (Ashkenazy *et al.*, 2010) and the *B. subtilis* CcpA-HPr complex bound to a synthetic cre site (3OQN) as a starting structure, the level of amino acid sequence conservation amongst LacI transcriptional regulators was analyzed. CcpA is colored according to the level of conservation within the LacI family of transcriptional regulators, while the DNA is colored yellow. Dark purple indicates 100% conservation, while blue indicates extensive sequence variation. (b) Sequence logo diagrams representing the abundance and position of nucleotides in the CcpA-regulated genes of *L. lactis* MG1363. (c) Changes in relative binding free energy upon substitutions at Met19 in CcpA as calculated by molecular dynamics. The reported errors of the relative free energies are standard errors of the mean. (d) Binding of CcpA to *cre* sites *in vitro*. The binding of CcpA-Met[19] and CppA-Ile[19] was tested with DNA sequences identified as *cre* sites upstream of *ptcB* and *mtlD* as

12

282   well as a perfect *cre* site. As a negative control the CodY recognition site upstream of *oppD*
283   was also tested (See also Supplementary Figure 10).
284
285   The effect of either the Ile or Thr substitution at position 19 was first investigated by

286   calculating the relative binding free energies of CcpA to a canonical *cre* site (Schumacher *et*

287   *al.*, 2011). The Ile variant had a more negative free energy of binding as compared to the wild

288   type protein, whereas the Thr variant did not exhibit significantly different binding to the

289   wild type protein. We then tested the effect of the DNA sequence on the binding free energy

290   for wild type and evolved CcpA, using structures derived from CcpA bound to two different

291   *cre* site sequences (3OQO and 3OQM) (Schumacher *et al.*, 2011). When the Ile was present

292   at position 19, tighter binding to all DNA sequences tested was computed, irrespective of the

293   starting structure used.

294   *Population dynamics of prolonged cultivation experiments*

295   The frozen population stocks, collected periodically throughout the prolonged cultivations,

296   served as snapshots of the adaptive evolution process to the chemostat environment. By

297   determining the abundance of the CcpA-Ile19 variant in stocks collected at different

298   generations, we were able to unravel the wash-in dynamics that outcompeted the native

299   CcpA-Met19. Quantification was carried out using pyrosequencing of the region containing

300   the SNP in the *ccpA* locus. The CcpA-Ile19 variant emerged after 50 generations in the

301   evolved populations and became dominant already by generation 150 (Supplementary Figure

302   11). While Met is encoded by ATG, Ile can be encoded by ATA, ATC or ATT. However,

303   only the first two codons were identified in the D=0.5 h^{-1} evolution experiment, with the

304   ATA mutant emerging prior to ATC (Supplementary Figure 12). At generation 309, when the

305   experiment was stopped, over 97% of the population carried the CcpA-Ile19 variant.

306   We then tested whether the phenotypic changes imposed by the CcpA mutation would be

307   sufficient to explain the wash-in kinetics observed using the glycerol stocks. For this purpose,

308   a simple model of chemostat growth with two competing strains was used to simulate the

309　prolonged experiment at a D of $0.5h^{-1}$. The model was able to accurately fit the observed

310　population dynamics, suggesting that the underlying mechanism can be fully understood in

311　terms of chemostat wash-in kinetics and is attributable to the mutant CcpA regulator

312　(Supplementary Figures 13A-C). Sensitivity analysis of this model showed that two pairs of

313　parameters cannot be estimated independently, only their ratios (Supplementary Figures 13D-

314　E). These are (i) the Monod constants (K_s) of the parent (Genr0) and the evolved (309C1-C4)

315　strains and (ii) the biomass yield of the parent strain and the emergence frequency of the fitter

316　strain. This uncertainty has, however, no implications for the conclusions derived from the

317　model. Another important aspect emerged from analyzing the model: the cells evolved at a

318　$D=0.5h^{-1}$ are predicted to outcompete Genr0 at any constant dilution rate not higher than μ_{max}.

319　*Parallel laboratory evolution and competition experiments under chemostat conditions at*

320　*different dilution rates*

321　We next addressed whether the fitness effect of the CcpA-Ile19 variant is dependent on

322　growth rate. We performed new evolution experiments in the chemostat environment at a

323　dilution rate of $0.6h^{-1}$, since at a D closer to μ_{max} (~0.67 h^{-1}), the concentration of limiting

324　nutrient becomes higher (Goel, Eckhardt, Puri, Jong, Branco dos Santos, Giera, Fusetti, Vos,

325　Kok, Poolman, Molenaar, Kuipers and Teusink, 2015), hence modulating the strength of the

326　selection pressure applied. Experiments were carried out for as many as 800 volume changes,

327　in a similar fashion as was done for the D of $0.5h^{-1}$. Sanger sequencing of the *ccpA* locus

328　from fragments, obtained by PCR using the frozen stocks as templates, indicated that indeed

329　the CcpA-Ile19 substitution was washing in as predicted by the model. Re-sequencing of the

330　whole-genome of single isolates of each of the populations evolved at $0.6h^{-1}$ revealed that

331　once again the only mutation that was consistent across all isolates was located in residue 19

332　of CcpA. This time all possible codons that encode Ile were found, suggesting that the amino

333　acid substitution is the only factor that confers a strong fitness benefit.

334   We further tested whether the same mutation is also advantageous for dilution rates that are

335   far lower than μ_{max} by performing competition experiments in chemostats between Genr0 and

336   309C1 (harboring only the CcpA-Met19 mutation). We used our growth model parameterized

337   with the data from the evolution experiments at a D of $0.5h^{-1}$, to simulate the population

338   dynamics of competition experiments carried out at a D of 0.2 and $0.3h^{-1}$ (Figure 5). Based on

339   this, we designed and performed the experiments, in which a small fraction (~10%) of cells

340   from a steady-state culture of 309C1 were mixed with a steady-state culture of Genr0

341   maintained at the same D. The population dynamics of these mixed cultures were monitored

342   in time by collecting samples from the culture effluent, and determining relative fractions

343   using pyrosequencing as before. We found an excellent agreement between experimental data

344   and model simulations (Figure 5), indicating that the fitness benefit of the CcpA-Met19

345   mutation is growth-rate independent.

346
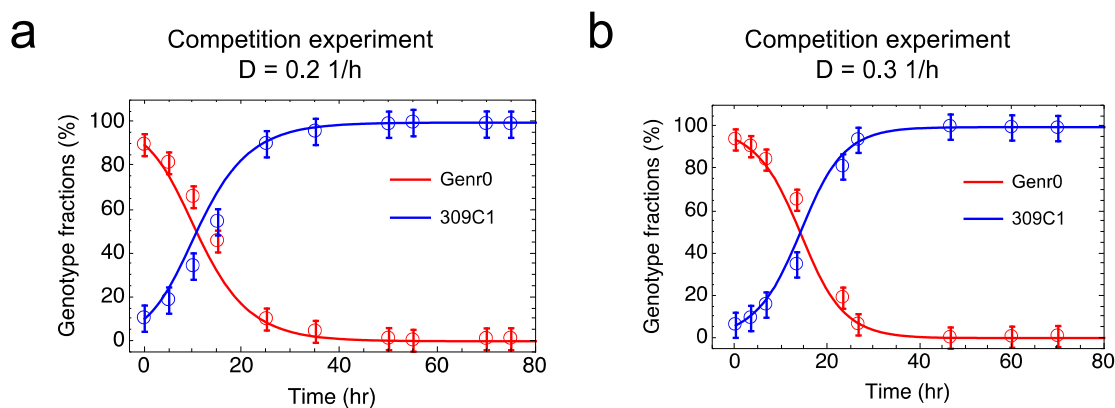
347

348   **Figure 5. Chemostat competition experiments.** Experiments were carried out between
349   Genr0 (red) and 309C1 (blue) at a dilution rate of 0.2 h^{-1} (panel a) and 0.3 h^{-1} (panel b).
350   Marks represent averages and standard deviations based on experimental data. Line depicts
351   results from *in silico* simulations using the model presented here parameterized based on the
352   population dynamics observed during the evolution experiments at a D = 0.5 h^{-1}
353   (Supplementary Figure 13).

354

355

356 **DISCUSSION**

357 *Replicate chemostats show high evolvability and low plasticity*

358 We studied the molecular mechanism of the adaptive strategy employed by *L. lactis* during

359 growth in a glucose-limited chemostat. In this way, we kept the identity of the selective

360 pressure constant, but varied its strength by imposing different dilution rates. Miniature

361 chemostats were constructed and growth medium and protocols developed that allowed

362 highly standardized, parallel and stable conditions for evolutionary studies in quadruplicate

363 for hundreds of consecutive generations, providing true biological replicates of this early

364 evolutionary process.

365 Intriguingly, we found rapid fixation of exactly the same beneficial amino-acid substitution

366 across all parallel evolutionary experiments, independent of growth rate. This demonstrates a

367 high evolvability with low evolutionary plasticity under these conditions. Evolutionary

368 plasticity is related to the existence of alternative mutations that give rise to a comparable

369 fitness enhancement for a particular selective pressure (Snell-Rood *et al.*, 2010; Forsman,

370 2014). Plasticity is high when many alternatives exist. Evolvability considers the rate of

371 evolution. It is both related to the number of mutations required, and their fixation rate, to

372 reach a specific quantitative change in fitness. If several mutations are required in sequence

373 for a specific quantitative change in fitness then evolvability is low, and vice-versa.

374 Evolvability can be assessed by determining the number of generations that it takes fitter

375 mutants to fix (Colegrave and Collins, 2008; Pigliucci, 2008). High plasticity and high

376 evolvability occur when alternative mutants fix at similar rates. High evolvability can also

377 occur at low plasticity: then one mutation fixes across replicates and dilution rates. The latter

378 was clearly the case in our study, and it appears that there is a single-peaked fitness

379 landscape, suggesting a strong preference for this specific mechanism, independent of the

16

380   strength of the selection pressure. As we will discuss shortly, our data suggest that alleviating

381   constraints on membrane occupancy may be that mechanism.

382   *Mutation in a global regulator rather than specifically in a glucose transporter*

383   In the chemostat, fitter mutants outgrow their competitors because they can grow at a rate

384   equal to the dilution rate, but at a lower concentration of the limiting nutrient (Gresham and

385   Hong, 2014; Bachmann *et al.*, 2016; Wortel *et al.*, 2016). So, in glucose-limited chemostats,

386   one expects enhanced selective pressure toward increased efficiency of glucose uptake, which

387   could be achieved by mutating or elevating the expression of high-affinity transport systems,

388   as previously observed (Bachmann *et al.*, 2012; Solopova *et al.*, 2012). However, although

389   glucose transport activity did increase, we found a mutation with pleiotropic effects in the

390   global carbon metabolism regulator CcpA, rather than in any of the three glucose

391   transporters.

392   The DNA binding domain of CcpA is highly conserved and in natural isolates of *L. lactis,* as

393   well as in CcpA homologues of other Gram-positive organisms such as *B. subtilis,* the Met

394   residue is present at an equivalent position. Based on the high-resolution structures of CcpA

395   from *B. subtilis*, this residue directly interacts with the nucleobases in the

396   *ackA2* and *glntR* promoter sequences but not with the synthetic *cre* site (Schumacher *et al.*,

397   2011). Whether CcpA binds with a higher or lower affinity to certain *cre* sites has been

398   investigated in *B. subtilis* (Marciniak *et al.*, 2012). While the focus was on the *cre* site

399   sequence itself, our study gives insights into the effect of the CcpA amino acid sequence on

400   DNA binding. The direct-binding data show that the effect of the amino acid substitution

401   consistently results in a tighter binding of CcpA to *cre* sequences, although not always to the

402   same extent. Other factors such as distance of the *cre* site to the transcriptional start site,

403   and/or the presence of other transcriptional regulators governing the expression of the operon

404   are known to affect gene expression (Deutscher, Francke and Postma, 2006). The different

405   extent of tighter binding of the evolved CcpA, in conjugation with the different regulatory

406   effects that CcpA may adopt for different operons, results in the reprogramming of the this

407   regulon, particularly around membrane proteins (underlying reasons are addressed below).

408   This allows the overall fine-tuning rather than the optimization of a particular trait (e.g.

409   increasing Ks of a single transporter), in response to imposed selection pressure.

410   CcpA was not the only global regulator to accumulate mutations. We also found a Phe

411   substitution for Ile^{214} in the DNA binding domain of CodY, a global regulator of nitrogen

412   metabolism in *L. lactis*. This mutation was only found in one chemostat but, similar to the

413   mutation accumulated in *ccpA,* indicates a strategy of modulation of global gene expression

414   in response to the culture conditions.

415   *Fitness enhancement independent from growth rate requires phenotypic plasticity*

416   The fact that we find a single mutation and that we can capture the population dynamics of

417   the CcpA-Met19 allele wash-in at different dilution rates with a simple growth model with

418   fixed kinetics, shows that the mechanism underlying the adaptation to a constant glucose-

419   limiting environment is independent of the growth rate. Yet different growth rates do require

420   different fluxes of glucose uptake, catabolism and biosynthesis. In view of the prevailing

421   perspective of growth-rate dependent regulation of the proteome, including global regulatory

422   mechanisms that may depend on this flux (Kotte, Zaugg and Heinemann, 2010; Basan *et al.*,

423   2015), this is far from trivial. This seems only possible if the cells possess a form of non-

424   genetic phenotypic plasticity that tolerates the adjustment of the gene-regulatory circuitry

425   under different conditions. A recent functional genomics study of the parent Genr0 strain at

426   different growth rates – using the same standard cultivation conditions – indeed suggests that

427   regulation at the metabolic level is the dominant form of phenotypic plasticity (Goel,

428   Eckhardt, Puri, Jong, Branco dos Santos, Giera, Fusetti, Vos, Kok, Poolman, Molenaar,

429   Kuipers and Teusink, 2015), *i.e.* the proteome of *L. lactis* hardly changed in the wide range of

430   growth rates also studies here $(0.2 - 0.6 \text{ h}^{-1})$. The presence of such metabolic phenotypic

431   plasticity seems therefore a requirement for our finding of low genetic plasticity and high

432   evolvability. It shows that the intracellular proteome does not impose major constraints on the

433   organism under these conditions, but rather the proteome of the membrane, as we will discuss

434   next.

435   *Reprogramming of gene expression hints at an important constraint at the level of membrane*

436   *occupancy*

437   While the mutation in CcpA does increase the expression of genes for high affinity glucose

438   PTS systems (e.g. PTS$^{\text{Man}}$), it simultaneously downregulates the expression of unused

439   membrane proteins such as transporters for other sugars and respiratory proteins. This dual

440   role was shown experimentally to indeed result in evolved cells with a more efficient glucose

441   uptake, and suggests that the most successful adaptation to constant glucose-limitation in *L.*

442   *lactis* requires reprogramming of membrane occupancy, not only upregulation of the specific

443   transporter. The idea that constraints related to limited resources and physicochemical

444   properties affect evolutionary strategies and create trade-offs is much under debate in recent

445   literature (Molenaar *et al.*, 2009; Scott *et al.*, 2014; Goel, Eckhardt, Puri, Jong, Branco dos

446   Santos, Giera, Fusetti, Vos, Kok, Poolman, Molenaar, Kuipers, Teusink, *et al.*, 2015;

447   O'Brien, Utrilla and Palsson, 2016). One interpretation of our data is that the down-regulation

448   of membrane processes provides more membrane space for glucose transporters, in analogy

449   with re-allocation of cytosolic proteins, as happens in *E coli* under different growth

450   conditions (Hui *et al.*, 2015).

451   Our results are consistent with a detailed computational study of *E. coli* that suggested the

452   presence of different growth regimes with different constraints limiting growth rate (O'Brien

453   *et al.*, 2013). At low growth rates, nutrient uptake was assumed to be the dominant constraint,

454   and cytosolic protein machinery for growth is in excess; only at nutrient excess, internal

455   proteome constraints became dominant. Such excess of cytosolic proteins at sub-maximal

456   growth can explain the predominantly metabolic regulation of flux under our conditions, and

457   hence explains the required phenotypic plasticity (Goel, Eckhardt, Puri, Jong, Branco dos

458   Santos, Giera, Fusetti, Vos, Kok, Poolman, Molenaar, Kuipers and Teusink, 2015). We thus

459   provide an experimental case-study that suggests that indeed uptake constraints are the main

460   constraint for fitness in the chemostat, and that global regulators may be able to overcome

461   them, through pleiotropic effects.

462   In line with this, we found that the growth rate of the CcpA-Met19 mutant was lower than in

463   wildtype when grown in batch (glucose excess), despite higher glucose uptake capacity -

464   something that is rather common for microorganisms evolved to nutrient-limited conditions

465   (Gresham and Hong, 2014). Also serial batch growth of *L. lactis* in emulsion– a method to

466   select for high cell number – selected for a mutation in the glucose transporter itself, rather

467   than in a regulator thereof (Bachmann *et al.*, 2013). In that case, the mutation reduced

468   glucose transport activity, thereby mimicking a low-glucose environment associated with

469   acetogenic metabolism, a high ATP-yield strategy.

470   In conclusion, our work shows that evolution to constant growth conditions can be mediated

471   by global regulators such as the carbon catabolite protein CcpA. Metabolic engineering

472   through the mutation of global regulators was first demonstrated by Stephanopoulos and

473   coworkers (Moxley *et al.*, 2009). We here show that the subtle manipulation of global

474   regulators to change entire metabolic networks is a strategy already employed by nature.

475

476   **MATERIAL AND METHODS**

477   ***Bacterial strains, media and growth conditions -*** *Lactococcus lactis* subsp. *cremoris*

478   MG1363 was grown in a chemically defined medium developed for prolonged cultivation,

479   CDMPC (Supplementary Table 1). The major differences compared to previously published

480   chemically defined media for *L. lactis* (Thomas, Ellwood and Longyear, 1979; Poolman and

481   Konings, 1988; Jensen and Hammer, 1993) are (i) the implementation of standardized

482   procedures that reduce variations between media batches, (e.g. safeguarding solubility); (ii)

483   the removal of components that are redundant or cause technical (downstream) difficulties or

484   perturbation of cell behavior; and (iii) careful tuning of the concentration of medium

485   compounds. The media consists of a phosphate buffer at pH 6.5, supplemented with all 20

486   amino acids, the vitamins biotin, DL-6,8-thioctic acid, D-pantothenic acid, nicotinic acid,

487   pyridoxal hydrochloride, pyridoxine hydrochloride and thiamine hydrochloride, and trace

488   metals $(NH_4)_6Mo_7O_{24}$, $CaCl_2$, $CoSO_4$, $CuSO_4$, $FeCl_2$, $MgCl_2$, $MnCl_2$ and $ZnSO_4$. Glucose was

489   added to a final concentration of 25 mM and cultivation was performed under an anaerobic

490   headspace. In order to study the effects of long term cultivation under constant conditions, *L.*

491   *lactis* MG1363 was cultivated in 4 chemostats run in parallel at 30°C at the following dilution

492   rates: $0.5\ h^{-1}$ for a total of 309 consecutive volume changes; $0.6\ h^{-1}$ for over 800 consecutive

493   volume changes. A small sample was removed every 10-15 generations and stored at -80 °C

494   in 20% (v/v) glycerol. In addition, the effluent was collected for optical density at 600 nm

495   (OD_{600}) measurements and HPLC analysis.

496   For subsequent studies, the glycerol stocks were used. 5 ml of fresh CDMPC was inoculated

497   from the frozen glycerol stocks and grown for 16 h at 30°C. The overnight culture was

498   subsequently diluted to a starting OD_{600} of 0.025-0.050 in either CDMPC or M17 medium

499   (Oxoid, Basingstoke, United Kingdom) supplemented with 0.5% (w/v) glucose or other

500   carbon sources as indicated.

501   ***Chemostat competition experiments between Genr0 and 309C1*** – The growth model

502   parameterized using the data from the evolution experiments at a D of 0.5h-1 was used to

503   designed the experiments, such that the initial fraction and sampling time-scheme would be

504   adequate to capture the predicted wash-in kinetics of the evolved cells. Actual competition

505   experiments were preceded by running four-parallel chemostats for 10 volume changes as

506   described above for Ds of 0.2 and 0.3h-1. Of the four steady states independently established

507   for each D, three included Genr0 and one 309C1. The competition stage was then initiated by

508   transferring the 309C1 culture into the Genr0 steady states such that they made up ~10% of

509   the population. After proper mixing a population sample is taken and considered to be t0.

510   Subsequently, and according to a predetermined sampling scheme, samples are removed from

511   the chemostat effluent. The relative fractions of the population corresponding to Genr0 and

512   309C1 were then determined in time resorting to pyrosequencing the *ccpA* locus (detailed in

513   the supplementary material).

514   ***Whole-genome sequencing and mutation detection*** – DNA was extracted from the *L. lactis*

515   single isolates using the GenElute^{TM} Bacterial Genomic DNA kit (Sigma-Aldrich, St. Louis,

516   MO, USA) according to the manufacturer's instructions except that the cells were first pre-

517   treated with lysozyme at 10 mg/ml for 1 hour at 50ºC. The isolates were sequenced with

518   100bp single-end reads across one lane of an Illumina HiSEQ 2000 flow cell (Illumina). The

519   resulting reads were deposited in the NCBI-SRA database (PRJNA185994). Reads were

520   mapped to the reference genome of *L. lactis* ssp. *cremoris* MG1363 (GenBank accession

521   number AM406671) and mutations detected using the CLC BIO Genomic Work Bench Suit

522   4.5 (CLC BIO, Arhus, Denmark). The mutation lists were verified using PCR amplification

523   and subsequent Sanger sequencing.

524   ***Microarray analysis*** – For RNA extraction, all strains were grown in CDMPC to the mid-

525   exponential growth phase. Total RNA was isolated using the High Pure RNA isolation Kit

526   (Roche Applied Science) and the quality was tested using an Agilent Bioanalyzer 2100

527   (Agilent Technologies Netherlands BV). All procedure regarding microarrays were

528   performed as described previously (van Hijum *et al.*, 2003, 2005). Data was processed and

529   normalized using the Lowess method with Micro-Prep (van Hijum *et al.*, 2003) and lists of

530   significant gene expression changes were generated on the basis of a Bayes *p*-vale and

531   Benjamini Hochberg multiple testing corrections (Hochberg and Benjamini, 1990). The DNA

532   microarray data have been submitted to GEO with accession number GSE67657.

533   The expression data was further analyzed by the Rank Product analysis (Breitling *et al.*,

534   2004) using the software package R version 2.10.1. This generates a list of genes ranked

535   according to ln ratio and calculates a conservative estimate of the percentage of false

536   positives (pfp). Proteins with pfp values smaller than 0.05 (5%) were regarded as

537   differentially expressed. The lists of significant gene expression levels were subjected to

538   functional   class   analyses   supported   by   the   Genome2D   webserver

539   (http://server.molgenrug.nl). This results in a list of classes that are overrepresented in the

540   dataset supplied on the basis of a hypergeometrical distribution test. The data for the

541   functional   classes   was   derived   from   the   KEGG   public   data   base

542   (http://www.genome.jp/kegg/ko.html) and for regulons from PePPER (de Jong *et al.*, 2012).

543   *[^{14}C]-glucose uptake* - Glucose uptake was monitored in whole cells using [^{14}C]-labeled

544   glucose essentially as previously described (Gouridis *et al.*, 2015). Briefly, all strains were

545   grown in CDMPC and harvested at the mid-exponential growth phase, washed twice in ice-

546   cold KPi buffer (50 mM, pH 6.5) and resuspended in KPi buffer to an OD_{600} of 0.5. Uptake

547   assays were performed at 30°C with stirring. [^{14}C]-glucose was added to 100 μl cell

548   suspension aliquots to a final concentration of 1.2-200 μM (0.005 μCi). The reactions were

549   stopped by the addition of 2 ml of ice-cold 0.1 M LiCl and the samples were collected on

550   0.45μm pore-size cellulose nitrate filters (Schleicher and Schuell GmbH, Dassel, Germany).

551   The filters were again washed with 2 ml 0.1 M LiCl. The background was determined by

552   adding the radiolabeled substrate to the cell suspension immediately after the addition of 2 ml

553   of ice-cold LiCl, followed by filtering. The assays were performed in triplicate using cells

554   from two independent cultures.

555 *Electrophoretic mobility shift assays* – To determine the *cre* site DNA binding affinity of

556 CcpA, binding assays were performed with Cy3-labeled oligonucleotides. DNA

557 oligonucleotides were from Biolegio B.V. (Nijmegen, the Netherlands) with the (+) strand

558 labelled at the 5'end with Cy3 and the (-) strand unlabeled. The oligonucleotides were mixed

559 1:1, incubated at 98ºC for 3 minutes and allowed to cool slowly to room temperature to

560 facilitate annealing. The annealed DNA was used at 4 nM and added to binding buffer (20

561 mM Tris-HCl pH8, 100 mM KCl, 10 mM MgCl$_2$, 1 mM EDTA, 1 mM DTT, 5% glycerol)

562 with additional BSA to 40 µg/ml. CcpA was added to concentrations between 100 nM and

563 800 nM. The binding reaction was performed at 30 ºC for 20 minutes after which the samples

564 were mixed with 5 X gel loading buffer (0.25% bromophenol blue, 40% sucrose). The

565 samples were analysed by electrophoresis on 7.5% native polyacrylamide gels using a TBE

566 buffer (90 mM Tris, 90 mM Boric Acid, 2 mM EDTA pH8.0). The fluorescent-labelled

567 oligonucleotides were visualised on a LAS-4000 imager (Fujifilm).

568 *Molecular dynamics simulations* - The simulated structures were based on the crystal

569 structures of CcpA bound to different DNA sequences by Schumacher *et al*. (Schumacher *et*

570 *al.*, 2011). Homology models of *L. lactis* proteins were created using the Swiss Model Server

571 (Arnold *et al.*, 2006). The sequence identity of the DNA binding domain in proteins from *B.*

572 *subtilis* and *L. lactis* is 77 % and only this region of the protein was used for the simulation.

573 Structures with differing DNA sequences were produced by fitting the differing bases to a

574 crystal structure before equilibrating the system. The protein domains after residue 64 were

575 removed from the simulation system and a harmonic bond with a 1000 kJ/(mol nm^2) force

576 constant was set between the backbone atoms of the last residues to restrain the structure of

577 the remaining domains. Each system was solvated in a dodecahedron box where each face of

578 the box was at least 1 nm from the protein and the DNA. This amounted in average to about

24

579   14500 water molecules, 130 Na^+ ions and 110 Cl^- ions, which corresponds to a 420 mM NaCl

580   solution and counter-ions.

581   All simulations were run using the Gromacs 4.5.5 (Hess *et al.*, 2008) simulation package. The

582   protein and DNA were modelled with CHARMM27 force field with CMAP corrections

583   (Foloppe and MacKerell Jr., 2000; MacKerell, Feig and Brooks, 2004) together with the

584   original TIP3P water model (Jorgensen *et al.*, 1983) as implemented in Gromacs 4.5.5.

585   Free energy changes were calculated from simulations using the Bennett acceptance ratio

586   method (Bennett, 1976) with the g_bar tool in Gromacs. Gromacs is a free software package

587   available at http://www.gromacs.org/. Relative free energies of binding were calculated using

588   a thermodynamic cycle described in Supplementary Figure 9.

589

596

597   **REFERENCES**

598   Arnold, K., Bordoli, L., Kopp, J. and Schwede, T. (2006) 'The SWISS-MODEL workspace:
599   a web-based environment for protein structure homology modelling', *Bioinformatics* , 22(2),
600   pp. 195–201. doi: 10.1093/bioinformatics/bti770.

601   Ashkenazy, H., Erez, E., Martz, E., Pupko, T. and Ben-Tal, N. (2010) 'ConSurf 2010:
602   calculating evolutionary conservation in sequence and structure of proteins and nucleic
603   acids', *Nucleic Acids Research* , 38(suppl 2), pp. W529–W533. doi: 10.1093/nar/gkq399.

604   Bachmann, H., Bruggeman, F. J., Molenaar, D., Branco dos Santos, F. and Teusink, B.

605 (2016) 'Public goods and metabolic strategies', *Current Opinion in Microbiology*, 31, pp.

606 109–115. doi: 10.1016/j.mib.2016.03.007.

607 Bachmann, H., Fischlechner, M., Rabbers, I., Barfa, N., Branco dos Santos, F., Molenaar, D.

608 and Teusink, B. (2013) 'Availability of public goods shapes the evolution of competing

609 metabolic strategies', *Proceedings of the National Academy of Sciences*, 110(35), pp. 14302–

610 7. doi: 10.1073/pnas.1308523110.

611 Bachmann, H., Starrenburg, M. J. C., Molenaar, D., Kleerebezem, M. and van Hylckama

612 Vlieg, J. E. T. (2012) 'Microbial domestication signatures of Lactococcus lactis can be

613 reproduced by experimental evolution', *Genome research*, 22, pp. 115–124. doi:

614 10.1101/gr.121285.111.

615 Barrick, J. E., Yu, D. S., Yoon, S. H., Jeong, H., Oh, T. K., Schneider, D., Lenski, R. E. and

616 Kim, J. F. (2009) 'Genome evolution and adaptation in a long-term experiment with

617 Escherichia coli.', *Nature*, 461(7268), pp. 1243–7. doi: 10.1038/nature08480.

618 Basan, M., Hui, S., Okano, H., Zhang, Z., Shen, Y., Williamson, J. R. and Hwa, T. (2015)

619 'Overflow metabolism in Escherichia coli results from efficient proteome allocation', *Nature*.

620 Nature Publishing Group, 528(7580), pp. 99–104. doi: 10.1038/nature15765.

621 Bennett, C. H. (1976) 'Efficient estimation of free energy differences from Monte Carlo

622 data', *Journal of Computational Physics*, 22(2), pp. 245–268. doi:

623 http://dx.doi.org/10.1016/0021-9991(76)90078-4.

624 Breitling, R., Armengaud, P., Amtmann, A. and Herzyk, P. (2004) 'Rank products: a simple,

625 yet powerful, new method to detect differentially regulated genes in replicated microarray

626 experiments', *FEBS Letters*, 573(1–3), pp. 83–92.

627 Buist, G., Kok, J., Leenhouts, K. J., Dabrowska, M., Venema, G. and Haandrikman, A. J.

628 (1995) 'Molecular cloning and nucleotide sequence of the gene encoding the major

629 peptidoglycan hydrolase of Lactococcus lactis, a muramidase needed for cell separation.',

630 *Journal of bacteriology*, 177(6), pp. 1554–63.

631 Castro, R., Neves, A. R., Fonseca, L. L., Pool, W. A., Kok, J., Kuipers, O. P. and Santos, H.

632 (2009) 'Characterization of the individual glucose uptake systems of Lactococcus lactis:

633 mannose-PTS, cellobiose-PTS and the novel GlcU permease', *Molecular Microbiology*.

634 Blackwell Publishing Ltd, 71(3), pp. 795–806. doi: 10.1111/j.1365-2958.2008.06564.x.

635 Colegrave, N. and Collins, S. (2008) 'Experimental evolution: experimental evolution and

636   evolvability.', *Heredity*. Nature Publishing Group, 100(5), pp. 464–470. doi:

637   10.1038/sj.hdy.6801095.

638   Dekel, E. and Alon, U. (2005) 'Optimality and evolutionary tuning of the expression level of

639   a protein', *Nature*, 436(7050), pp. 588–592.

640   Deutscher, J., Francke, C. and Postma, P. W. (2006) 'How phosphotransferase system-related

641   protein phosphorylation regulates carbohydrate metabolism in bacteria.', *Microbiology and*

642   *molecular biology reviews : MMBR*, 70(4), pp. 939–1031. doi: 10.1128/MMBR.00024-06.

643   Foloppe, N. and MacKerell Jr., A. D. (2000) 'All-atom empirical force field for nucleic acids:

644   I. Parameter optimization based on small molecule and condensed phase macromolecular

645   target data', *Journal of Computational Chemistry*. John Wiley & Sons, Inc., 21(2), pp. 86–

646   104. doi: 10.1002/(SICI)1096-987X(20000130)21:2<86::AID-JCC2>3.0.CO;2-G.

647   Forsman, A. (2014) 'Rethinking phenotypic plasticity and its consequences for individuals,

648   populations and species.', *Heredity*. Nature Publishing Group, 115(August), pp. 1–9. doi:

649   10.1038/hdy.2014.92.

650   Goel, A., Eckhardt, T. H., Puri, P., Jong, A., Branco dos Santos, F., Giera, M., Fusetti, F.,

651   Vos, W. M., Kok, J., Poolman, B., Molenaar, D., Kuipers, O. P. and Teusink, B. (2015)

652   'Protein costs do not explain evolution of metabolic strategies and regulation of ribosomal

653   content', *Molecular Microbiology*. doi: 10.1111/mmi.13012.

654   Goel, A., Eckhardt, T. H., Puri, P., Jong, A., Branco dos Santos, F., Giera, M., Fusetti, F.,

655   Vos, W. M., Kok, J., Poolman, B., Molenaar, D., Kuipers, O. P., Teusink, B., de Jong, A.,

656   Branco dos Santos, F., Giera, M., Fusetti, F., de Vos, W. M., Kok, J., Poolman, B., Molenaar,

657   D., Kuipers, O. P. and Teusink, B. (2015) 'Protein costs do not explain evolution of

658   metabolic strategies and regulation of ribosomal content', *Molecular Microbiology*, 97(1), pp.

659   77–92. doi: 10.1111/mmi.13012.

660   Görke, B. and Stülke, J. (2008) 'Carbon catabolite repression in bacteria: many ways to make

661   the most out of nutrients.', *Nature reviews. Microbiology*. Nature Publishing Group, 6(8), pp.

662   613–24. doi: 10.1038/nrmicro1932.

663   Gouridis, G., Schuurman-Wolters, G. K., Ploetz, E., Husada, F., Vietrov, R., de Boer, M.,

664   Cordes, T. and Poolman, B. (2015) 'Conformational dynamics in substrate-binding domains

665   influences transport in the ABC importer GlnPQ.', *Nature structural & molecular biology*.

666   Nature Publishing Group, a division of Macmillan Publishers Limited. All Rights Reserved.,

667   22(1), pp. 57–64. doi: 10.1038/nsmb.2929.

668   Gresham, D. and Hong, J. (2014) 'The functional basis of adaptive evolution in chemostats.',

669   *FEMS microbiology reviews*. The Oxford University Press, 39(1), pp. 2–16. doi:

670   10.1111/1574-6976.12082.

671   Hess, B., Kutzner, C., van der Spoel, D. and Lindahl, E. (2008) 'GROMACS 4: Algorithms

672   for Highly Efficient, Load-Balanced, and Scalable Molecular Simulation', *Journal of*

673   *Chemical Theory and Computation*, 4(3), pp. 435–447. doi: 10.1021/ct700301q.

674   van Hijum, S. A. F. T., de Jong, A., Buist, G., Kok, J. and Kuipers, O. P. (2003) 'UniFrag

675   and GenomePrimer: selection of primers for genome-wide production of unique amplicons ',

676   *Bioinformatics* , 19(12), pp. 1580–1582. doi: 10.1093/bioinformatics/btg203.

677   van Hijum, S., de Jong, A., Baerends, R., Karsens, H., Kramer, N., Larsen, R., den Hengst,

678   C., Albers, C., Kok, J. and Kuipers, O. (2005) 'A generally applicable validation scheme for

679   the assessment of factors involved in reproducibility and quality of DNA-microarray data',

680   *BMC Genomics*, 6(1), p. 77. doi: 10.1186/1471-2164-6-77.

681   Hochberg, Y. and Benjamini, Y. (1990) 'More powerful procedures for multiple significance

682   testing', *Statistics in Medicine*. Wiley Subscription Services, Inc., A Wiley Company, 9(7),

683   pp. 811–818. doi: 10.1002/sim.4780090710.

684   Hui, S., Silverman, J. M., Chen, S. S., Erickson, D. W., Basan, M., Wang, J., Hwa, T. and

685   Williamson, J. R. (2015) 'Quantitative proteomic analysis reveals a simple strategy of global

686   resource allocation in bacteria.', *Molecular systems biology*. EMBO Press, 11(1), p. 784. doi:

687   10.15252/msb.20145697.

688   Jensen, P. R. and Hammer, K. (1993) 'Minimal Requirements for Exponential Growth of

689   Lactococcus lactis.', *Applied and environmental microbiology*, 59(12), pp. 4363–6.

690   de Jong, A., Pietersma, H., Cordes, M., Kuipers, O. and Kok, J. (2012) 'PePPER: a webserver

691   for prediction of prokaryote promoter elements and regulons', *BMC Genomics*, 13(1), p. 299.

692   doi: 10.1186/1471-2164-13-299.

693   Jorgensen, W. L., Chandrasekhar, J., Madura, J. D., Impey, R. W. and Klein, M. L. (1983)

694   'Comparison of simple potential functions for simulating liquid water', *The Journal of*

695   *Chemical Physics*. AIP, 79(2), pp. 926–935. doi: 10.1063/1.445869.

696   Kotte, O., Zaugg, J. B. and Heinemann, M. (2010) 'Bacterial adaptation through distributed

697   sensing of metabolic fluxes.', *Molecular systems biology*. Nature Publishing Group, 6(355),

698   p. 355. doi: 10.1038/msb.2010.10.

699   Kuipers, O. P., de Jong, A., Baerends, R. J. S., van Hijum, S. A. F. T., Zomer, A. L., Karsens,

700   H. A., den Hengst, C. D., Kramer, N. E., Buist, G. and Kok, J. (2002) 'Transcriptome

701   analysis and related databases of Lactococcus lactis.', *Antonie van Leeuwenhoek*, 82(1–4),

702   pp. 113–22.

703   Lázár, V., Pal Singh, G., Spohn, R., Nagy, I., Horváth, B., Hrtyan, M., Busa-Fekete, R.,

704   Bogos, B., Méhi, O., Csörgő, B., Pósfai, G., Fekete, G., Szappanos, B., Kégl, B., Papp, B.

705   and Pál, C. (2013) 'Bacterial evolution of antibiotic hypersensitivity.', *Molecular systems*

706   *biology*. EMBO Press, 9(1), p. 700. doi: 10.1038/msb.2013.57.

707   Linares, D. M., Kok, J. and Poolman, B. (2010) 'Genome sequences of Lactococcus lactis

708   MG1363 (revised) and NZ9000 and comparative physiological studies.', *Journal of*

709   *bacteriology*, 192(21), pp. 5806–12. doi: 10.1128/JB.00533-10.

710   MacKerell, A. D., Feig, M. and Brooks, C. L. (2004) 'Improved Treatment of the Protein

711   Backbone in Empirical Force Fields', *Journal of the American Chemical Society*, 126(3), pp.

712   698–699. doi: 10.1021/ja036959e.

713   Marciniak, B. C., Pabijaniak, M., de Jong, A., Dűhring, R., Seidel, G., Hillen, W. and

714   Kuipers, O. P. (2012) 'High- and low-affinity cre boxes for CcpA binding in Bacillus subtilis

715   revealed by genome-wide analysis.', *BMC genomics*. BioMed Central, 13(1), p. 401. doi:

716   10.1186/1471-2164-13-401.

717   Meadows, A. L., Karnik, R., Lam, H., Forestell, S. and Snedecor, B. (2010) 'Application of

718   dynamic flux balance analysis to an industrial Escherichia coli fermentation.', *Metabolic*

719   *engineering*, 12(2), pp. 150–60. doi: 10.1016/j.ymben.2009.07.006.

720   Molenaar, D., van Berlo, R., de Ridder, D. and Teusink, B. (2009) 'Shifts in growth strategies

721   reflect tradeoffs in cellular economics.', *Molecular systems biology*. Nature Publishing

722   Group, 5(323), p. 323. doi: 10.1038/msb.2009.82.

723   Moxley, J. F., Jewett, M. C., Antoniewicz, M. R., Villas-Boas, S. G., Alper, H., Wheeler, R.

724   T., Tong, L., Hinnebusch, A. G., Ideker, T., Nielsen, J. and Stephanopoulos, G. (2009)

725   'Linking high-resolution metabolic flux phenotypes and transcriptional regulation in yeast

726   modulated by the global regulator Gcn4p ', *Proceedings of the National Academy of Sciences*

727   , 106(16), pp. 6477–6482. doi: 10.1073/pnas.0811091106.

728   Novick, A. and Szilard, L. (1950) 'Description of the Chemostat', *Science*, 112(2920).

729   O'Brien, E. J., Lerman, J. A., Chang, R. L., Hyduke, D. R. and Palsson, B. Ø. (2013)

730 'Genome-scale models of metabolism and gene expression extend and refine growth

731 phenotype prediction.', *Molecular systems biology*. European Molecular Biology

732 Organization, 9(693), p. 693. doi: 10.1038/msb.2013.52.

733 O'Brien, E. J., Utrilla, J. and Palsson, B. O. (2016) 'Quantification and Classification of E.

734 coli Proteome Utilization and Unused Protein Costs across Environments', *PLOS*

735 *Computational Biology*. Edited by C. D. Maranas. Public Library of Science, 12(6), p.

736 e1004998. doi: 10.1371/journal.pcbi.1004998.

737 Oliveira, A., Nielsen, J. and Förster, J. (2005) 'Modeling Lactococcus lactis using a genome-

738 scale flux model', *BMC microbiology*, 15, pp. 1–15. doi: 10.1186/1471-2180-5-39.

739 Pigliucci, M. (2008) 'Is evolvability evolvable?', *Nature reviews Genetics*. Nature Publishing

740 Group, 9(1), pp. 75–82. doi: 10.1038/nrg2278.

741 Poolman, B. and Konings, W. N. (1988) 'Relation of growth of Streptococcus lactis and

742 Streptococcus cremoris to amino acid transport', *J Bacteriol*. 1988/02/01, 170(2), pp. 700–

743 707.

744 Schumacher, M. A., Sprehe, M., Bartholomae, M., Hillen, W. and Brennan, R. G. (2011)

745 'Structures of carbon catabolite protein A-(HPr-Ser46-P) bound to diverse catabolite response

746 element sites reveal the basis for high-affinity binding to degenerate DNA operators.',

747 *Nucleic acids research*, 39(7), pp. 2931–42. doi: 10.1093/nar/gkq1177.

748 Scott, M., Klumpp, S., Mateescu, E. M. and Hwa, T. (2014) 'Emergence of robust growth

749 laws from optimal regulation of ribosome synthesis.', *Molecular systems biology*, 10, p. 747.

750 Scott, M., Mateescu, E. M., Zhang, Z. and Hwa, T. (2010) 'Interdependence of Cell Growth

751 Origins and Consequences', *Science*. American Association for the Advancement of Science,

752 330(November), pp. 1099–1102. doi: 10.1126/science.1192588.

753 Snell-Rood, E. C., Van Dyken, J. D., Cruickshank, T., Wade, M. J. and Moczek, A. P. (2010)

754 'Toward a population genetic framework of developmental evolution: The costs, limits, and

755 consequences of phenotypic plasticity', *BioEssays*. NIH Public Access, pp. 71–81. doi:

756 10.1002/bies.200900132.

757 Solopova, A., Bachmann, H., Teusink, B., Kok, J., Neves, A. R. and Kuipers, O. P. (2012) 'A

758 specific mutation in the promoter region of the silent cel cluster accounts for the appearance

759 of lactose-utilizing Lactococcus lactis MG1363.', *Applied and environmental microbiology*,

760 78(16), pp. 5612–21. doi: 10.1128/AEM.00455-12.

761   Thomas, T. D., Ellwood, D. C. and Longyear, V. M. (1979) 'Change from homo- to

762   heterolactic fermentation by Streptococcus lactis resulting from glucose limitation in

763   anaerobic chemostat cultures.', *Journal of bacteriology*, 138(1), pp. 109–17.

764   Wiser, M. J., Ribeck, N. and Lenski, R. E. (2013) 'Long-term dynamics of adaptation in

765   asexual populations.', *Science (New York, N.Y.)*, 342(6164), pp. 1364–7. doi:

766   10.1126/science.1243357.

767   Wortel, M. T., Bosdriesz, E., Teusink, B. and Bruggeman, F. J. (2016) 'Evolutionary

768   pressures on microbial metabolic strategies in the chemostat', *Scientific Reports*. Nature

769   Publishing Group, 6, p. 29503. doi: 10.1038/SREP29503.

770

771

a

ptcB ptcA llmg_0439   ptnD   ptnC   ptnAB   glcU

PTS^{Cel} low affinity   PTS^{Man} high affinity   Glucose permease
Km = 8.7 mM   Km = 13 µM   Km = 2.4 mM

b

Strain	Glucose uptake and metabolism	
	Vmax (nmol/min x mg protein)	Km (µM)
Genr0	176.0 ± 13.1	21.0 ± 0.8
309C1	484.7 ± 37.2	22.2 ± 0.7

a variable — conserved

b
all *cre* sites
up regulated genes
down regulated genes
unchanged genes

c

cre site	Starting structure	DNA sequence	Relative free energy (kJ/mol)	K_D (Genr0)/ K_D (variant)
CcpA-Ile[19]				
perfect	3OQO	CTGTTAGCGCTTTCAG	-14.5 ± 2	350
deviant	3OQO	CTGTTAGCGCTTTAAG	-14.5 ± 2	350
	3OQM		-9.3 ± 3	43
ptcB	3OQO	TAGATAACGCTTACAT	-8.6 ± 3	32
	3OQM		-6.2 ± 3	12
mtlD	3OQO	ATGTAAAAGCTTACAA	-9.2 ± 2	41
	3OQM		-16.7 ± 2	810
CcpA-Thr[19]				
perfect	3OQO	CTGTTAGCGCTTTCAG	2.7 ± 2	0.3

d

CcpA variant	CcpA concentration at which binding is observed (µM)		
	cre site		
	perfect	*ptcB*	*mtlD*
CcpA-Met[19]	0.4	>1.6	0.4
CcpA-Ile[19]	0.1	0.4	0.2

a Competition experiment
D = 0.2 1/h
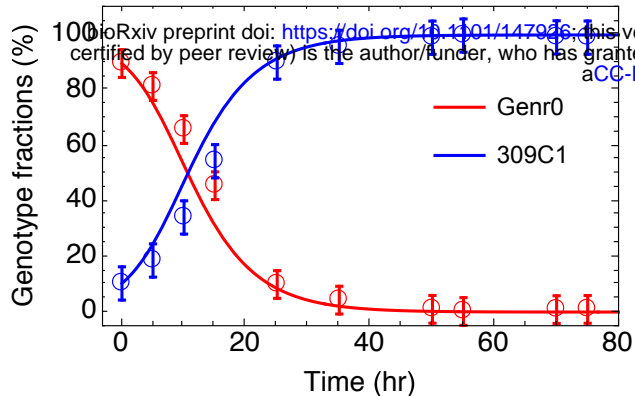
b Competition experiment
D = 0.3 1/h
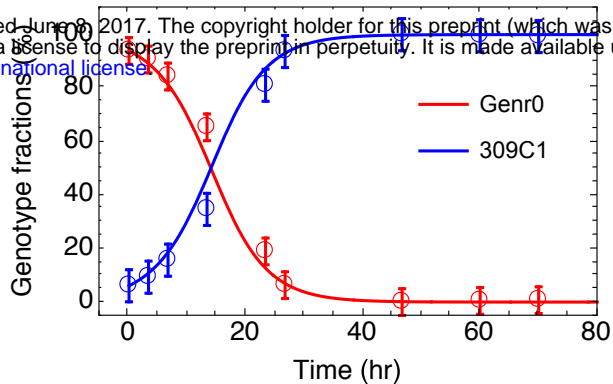
1 **Supplementary Information to:**

2 *Title:* Glucose-limitation in *Lactococcus lactis* shapes a single-peaked fitness landscape that

3 exposes membrane occupancy as a dominant constraint

4

5

6 *Authors:*

7 Claire E. Price[a,b,c,1,2], Filipe Branco dos Santos[c,d,e,2], Anne Hesseling[a], Jaakko J. Uusitalo[f],

8 Herwig Bachmann[c,d], Vera Benavente[d], Anisha Goel[c,d,3], Jan Berkhout[d], Frank J.

9 Bruggeman[d], Siewert-Jan Marrink[f], Manolo Montalban-Lopez[a], Anne de Jong[a], Jan Kok[a],

10 Douwe Molenaar[c,d], Bert Poolman[b], Bas Teusink[c,d], Oscar P. Kuipers[a,c]

11

12 *Author affiliations:*

13 [a] Molecular Genetics group, University of Groningen, Nijenborgh 7, 9747 AG Groningen, the

14 Netherlands

15 [b] Department of Biochemistry, University of Groningen, Nijenborgh 4, 9747 AG Groningen,

16 the Netherlands

17 [c] Kluyver Center for Genomics of Industrial Fermentations/NCSB, Julianalaan 67, 2628 BC

18 Delft, The Netherlands

19 [d] Systems Bioinformatics, Faculty of Earth and Life Sciences, VU University Amsterdam, De

20 Boelelaan 1085, 1081 HV Amsterdam, The Netherlands

21 [e] Molecular Microbial Physiology Group, Faculty of Life Sciences, Swammerdam Institute of

22 Life Sciences, University of Amsterdam, Science Park 904, Amsterdam 1098 XH,

23 Netherlands

24 [f] Molecular Dynamics group, University of Groningen, Nijenborgh 7, 9747 AG Groningen,

25 the Netherlands

26

27 *Author footnotes:*

28 [1] Current address: DSM Biotechnology Centre, Alexander Fleminglaan 1, 2613 AX, Delft,

29 The Netherlands

30 [2] Both authors contributed equally

31 [3] Current address: Chr. Hansen, Boege Allé 10-12, 2970 Hoersholm, Denmark

32

33 *Corresponding authors:* b.teusink@vu.nl and o.p.kuipers@rug.nl

34

35   **Supplementary Results**

36   *Mutations in all sequenced strains compared to published sequences*

37   The sequences of Genr0 and the evolved strains were compared to those published for *L.*

38   *lactis* MG1363. All strains contained a mutation in *malR* which would results in a frameshift

39   in the maltose operon transcriptional repressor MalR. This could be due to sequencing errors

40   from adjacent C nucleotides or a truncated MalR protein. The truncation would result in a

41   HTH DNA binding domain without a ligand-binding domain.

42

43   *Mutations unique to strains 309C2, 309C3 and 309C4*

44   The effect of the mutations identified in *rpoC* in 309C2 and *greA* in 309C4 on transcriptional

45   fidelity were investigated using *lacZ* constructs with a premature stop codon at position Glu[13]

46   (P. Gamba and J.W. Veening, unpublished data). However, β-galactosidase activity was

47   similar in the evolved strains and the original strains Genr0 and *L. lactis* MG1363

48   (Supplementary Figure 2), indicating that in the evolved strains, RNA polymerase and

49   elongation factor function as they do in wild type strains.

50   Since proteins encoded by llmg_1597, a hypothetical protein possibly with RNA-binding

51   function, and *llrF,* a two-component system regulator, are not well-characterized, no

52   prediction as to change or function could be made for the mutations identified. In contrast,

53   CodY is a well-studied transcriptional regulator of nitrogen metabolism and based on

54   structural studies it can be predicted that the SNP identified results in a Phe substitution for

55   Ile[214] in the DNA binding domain (Levdikov, Blagova, Joseph, Sonenshein, & Wilkinson,

56   2006). The absence of a high-resolution structure of CodY bound to a DNA operator makes

57   any further prediction of the effect on DNA binding difficult.

58   A number of SNPs were predicted to lie in non-coding regions at positions that lie in or near

59   putative promoter sequences, thus making predictions as to the effect of such mutations

60   difficult.   The SNP at position 490263 resulted in an altered ribosomal binding site

61   (GGAGGA to GGAGAA) upstream of the gene for a Hu-like DNA binding protein, *hllA*.

62   This could suggest that a modest reduction of the translation of this mRNA, encoding a

63   putative DNA-binding protein, could take place.

64

65   *Global gene expression patterns of evolved strains*

66   The evolved strains were revived in CDMPC and grown until mid-exponential phase at

67   which microarray analysis using in-house *L. lactis* MG1363 slides (Kuipers et al. 2002) was

2

68   performed. Gene expression in the evolved strains was compared to that of Gen0. A total

69   number of 377 genes exhibited changed expression in the evolved strains (Supplementary

70   Table 4). Approximately a third of the changes were in at least 3 of the 4 strains. Altered gene

71   expression was dominantly in genes involved in membrane transport, especially carbohydrate

72   import (Supplementary Figure 3A, Supplementary Table 3, Supplementary Table 4).

73   Regulon analysis of the differentially expressed genes revealed that CcpA-regulated genes

74   were over-represented in the data set. For strain 309C4, those regulated by CodY were

75   prevalent as well (Supplementary Figure 3B, Supplementary Table 3).

76   CcpA controls the preferential use of glucose over other sugars (Deutscher et al. 2006),

77   including expression of sugar uptake systems such as those for glucose. Transcriptome

78   analysis of all the evolve strains revealed similar patterns of expression and increased glucose

79   uptake (Supplementary Figure 3C and D).

80   The ability to utilize other carbon sources was diminished for the evolved strains

81   (Supplementary Figure 4A) in accordance with the down regulation of, amongst others, genes

82   encoding for maltose transporters, ABC sugar import systems and sugar utilization enzymes

83   in the microarray data (Supplementary Table 3). Many of these genes are CcpA-regulated.

84

85   ***Phenotypic characterization of evolved strains to identify effects of transcriptional***

86   ***regulation.***

87   The strains were not only adapted to the constant culture conditions through expression

88   changes in carbohydrate uptake and utilization systems, but also through changes in the

89   expression levels of genes involved in amino acid uptake and metabolism. Ordinarily, *L.*

90   *lactis* MG1363 grows faster when amino acids are taken up as oligopeptides than when only

91   free amino acids are available (Supplementary Figure 5B). This is due to the efficient import

92   of oligopeptides by the major oligopeptide transporter Opp (Detmers et al., 2000).

93   Cultivation in free amino acids led to the down regulation of the entire *opp* operon

94   (Supplementary Figure 5A) and the cells were as a result impaired in growth on oligopeptide

95   containing medium (Supplementary Figure 5B and C). The difference in growth in

96   oligopeptide-containing medium between the evolved strains and Genr0 is well correlated

97   with the expression levels of the *opp* operon except in the case of 309C4. In this strain the

98   down regulation of the *opp* operon appears to be partially compensated for by the

99   concomitant up regulation of the analogous *opp2* operon. This operon was previously

100   thought to be cryptic in *L. lactis* MG1363 (Sanz et al. 2004), but in our evolved strain is

101   expressed and OppA2 was detected using mass spectrometry (data not shown).

102   Prolonged cultivation under an anaerobic atmosphere had a dramatic effect on the ability of

103   the evolved strains to utilize the electron transport chain present in *L. lactis*. *L. lactis* is

104   unable to synthesize heme *de novo,* but if heme is added to the growth medium, the bacterium

105   can synthesize the cytochromes needed for the generation of a proton motive force (PMF)

106   and subsequent ATP synthesis at the membrane-embedded ATP synthase (Brooijmans et al.

107   2007). This results in an increase in biomass (Cesselin et al. 2001) as observed for Genr0

108   (Supplementary Figure 6). The evolved strains did not show any increase in biomass upon

109   addition of heme to the medium and expression data showed the down regulation of a number

110   of NADH oxidases/dehydrogenases (Supplementary Table 3) which are likely to be

111   responsible for the inability of these strains to respire.

112   In addition the evolved strains displayed a well-characterized long-chain phenotype

113   associated with a deficiency in the major autolysin AcmA (Supplementary Figure 7) (Buist et

114   al. 1995). The expression of the *acmA* gene was down regulated in all the evolved strains

115   (Supplementary Table 3) and in agreement with the down regulation of the *acmA* gene, the

116   evolved cells were less prone to lysis in the stationary growth phase (Supplementary Figure

117   7).

118

Effect of M19I mutation on the binding affinity of CcpA

120   The effects of the *ccpA* mutations were investigated using homology modeling, molecular

121   dynamic simulations and *in vitro* binding assays using purified CcpA from the mutated

122   strains. The high-resolution structure of *B. subtilis* CcpA was used to model *L. lactis* CcpA

123   (Figure 4A and Supplementary Figure 8) (Schumacher et al. 2011) since the one published

124   for *L. lactis* CcpA lacks the N-terminal DNA-binding domain (Loll et al. 2007). The structure

125   from *B. subtilis* includes CcpA bound to the DNA catabolic response element (*cre* site) as

126   well as the activating phosphoprotein HPr. Met19 is located in the second helix contained in

127   the DNA binding domain. The methionine at this position is highly conserved across all

128   Gram-positive CcpA proteins sequenced to date and in 4 natural isolates of *L. lactis* for which

129   the *ccpA* locus was resequenced (Supplementary Table 6).

130   The binding of CcpA from Genr0 and 309F1 to 4 DNA operators was examined: synthetic

131   *cre* sites, *cre* site upstream of *ptcB*, *cre* site upstream of *mtlD* and, as a negative control, the

132   CodY binding sequence upstream of *oppD* (Figure 4D and Supplementary 10), representing

133   genes that are down regulated as well as up regulated in the evolved strains. For all the cre

134   sites tested, the CcpA-Ile19 variant showed an increase in binding affinity for the DNA

135   operators tested. This was most pronounced for the sequence upstream of *ptcB* and least

136   pronounced for *mtlD*.

137

138   *Evolution of Ccp-Thr[19] variant*

139   The appearance of and subsequent dominance of the *ccpA* mutations was tracked in time

140   during the evolution experiment through PCR amplification of the *ccpA* locus from the frozen

141   stocks. The PCR products were resequenced using traditional Sanger sequencing, with

142   manual chromatogram inspection, as well as pyrosequencing, which allows for the

143   quantitation of SNPs in a population. In addition, frozen stocks were streaked onto CDMPC

144   agar plates and the *ccpA* locus was PCR amplified and resequenced from single colonies. The

145   CcpA-Ile[19] variant emerged around 50 generations in the evolved strains and by generation

146   150 was the dominant population in the chemostat (Supplementary Figure 11 and 12). The

147   pattern of emergence was different for strain 309C4, with the emergence of a second variant,

148   i.e. CcpA-Thr[19]. This variant was only detected after 250 generations and by 309 generations

149   both CcpA variants existed in the population. Sequencing of numerous single colony isolates

150   could not detect any wild type *ccpA* by 300 generations (data not shown).

151   Sequencing of single colony isolates from the C4 frozen stocks, revealed that the unique

152   CcpA-Thr[19] variant is linked to the CodY-Phe[214]. At 309 generations the only combinations

153   identified were CcpA-Ile[19] and CodY-Ile[214] (i.e. wild type CodY) and CcpA-Thr[19] and CodY-

154   Phe[214]. Stocks resequenced from earlier in the evolution experiment also contained CcpA-

155   Thr[19], CodY-Ile[214] pairs, indicating that the *codY* mutations occurred in the unique CcpA-

156   Thr[19] background.

157

158   *Model description and parameter estimation*

159   The differential equations describing the rates of the change in the limiting nutrient

160   concentration (s) and the biomass concentrations of the wild type (w) and the mutant (m) are,

161

$$\frac{ds}{dt}(t) = D\big(s_r - s(t)\big) - \frac{\mu_w}{Y_w}w(t) - \frac{\mu_m}{Y_m}m(t)$$

$$\frac{dw}{dt}(t) = (\mu_w - D)w(t)$$

$$\frac{dm}{dt}(t) = (\mu_m - D)m(t)$$

162 $\hspace{12cm}$ (1)

163 with: $\mu_w = \mu_w^{max}\frac{s(t)}{K_w+s(t)}$, $\mu_m = \mu_m^{max}\frac{s(t)}{K_m+s(t)}$, D as the dilution rate in h^{-1}, μ as the specific

164 growth rate in h^{-1}, Y is the biomass yield in gDW.mM^{-1}, μ/Y as the specific nutrient uptake

165 rate in mM.gDW^{-1}.h^{-1}, K as the Monod constant in mM, s_r as the vessel concentration of the

166 limiting nutrient in mM, s as the reactor concentration of the limiting nutrient in mM, and w

167 and m as the biomass abundances in gDW.L^{-1}. The subscripts "w" and "m" indicate whether

168 the parameter concerns the wild type or the mutant. Alternatively, we could have taken the

169 OD to represent the biomass concentration, which we now take as gDW.L^{-1}.

170 Considering the experimental data it is more convenient to consider a dimensional time

171 defined as $\tau = Dt$, which is what we call generations. With this definition we obtain,

172

$$\frac{ds}{d\tau}(\tau) = \left(s_r - s(\tau)\right) - \frac{\mu_w}{DY_w}w(\tau) - \frac{\mu_m}{DY_m}m(\tau)$$

$$\frac{dw}{d\tau}(\tau) = \left(\frac{\mu_w}{D} - 1\right)w(\tau)$$

$$\frac{dm}{d\tau}(\tau) = \left(\frac{\mu_m}{D} - 1\right)m(\tau)$$

173 $\hspace{12cm}$ (2)

174 Since we are considering the fixation of the mutant, the initial conditions are given by the

175 steady state of wild type in the absence of the mutant:

176

$$w(0) = Y_w\frac{D(K_w + s_r) - s_r\mu_w^{max}}{D - \mu_w^{max}}$$

$$s(0) = \frac{DK_w}{\mu_w^{max} - D}$$

177 $\hspace{12cm}$ (3)

178 Equations 2 and 3 were fitted against the experimental data. The results of the fit are shown

179 in Supplementary Table 1 and Supplementary Figure 13. These data indicate that observed

180 experimental data is in agreement with a basic chemostat model of the competitive growth of

181 two microorganisms. The values of the fitted parameters are not the only set of values that

182 describe the data. The data set is too small, and hence more variables would have to be

183 measured to obtain a unique estimation of parameter values.

184

185

186   Supplementary Table 7: Overview of parameters (fitted and experimental settings).

Parameter	Wild type (w)	Mutant (m)
Yield on substrate, Y (g/mM)	0.076	0.08
Maximal growth, μ^{max} (hr^{-1})	0.71	0.60
Monod constant, K (mM)	0.019	0.0033
	Experiment settings	
Dilution rate, D (hr^{-1})	0.5	
Reservoir substrate concentration, Sr (mM)	25	

187

Supplementary materials and methods

Chemically defined medium for prolonged cultivations

190   *Lactococcus lactis* subsp. *cremoris* MG1363 was grown in a chemically defined medium

191   developed for prolonged cultivation, CDMPC (Supplementary Table 1). The media consists

192   of a phosphate buffer at pH 6.5, supplemented with all 20 amino acids, the vitamins biotin,

193   DL-6,8-thioctic acid, D-pantothenic acid, nicotinic acid, pyridoxal hydrochloride, pyridoxine

194   hydrochloride and thiamine hydrochloride, and trace metals $(NH_4)_6Mo_7O_{24}$, $CaCl_2$, $CoSO_4$,

195     $CuSO_4$, $FeCl_2$, $MgCl_2$, $MnCl_2$ and $ZnSO_4$. The composition was based on the nutrient

196   requirements and biomass composition of *L. lactis* MG1363. The major differences compared

197   to previously published chemically defined media for *L. lactis* (Thomas et al. 1979; Poolman

198   and Konings 1988; Jensen and Hammer 1993) are (i) the removal of acetate and ammonium

199   ions; (ii) removal of redundant and/or unessential vitamins such as vitamin B_{12}, or those that

200   could in addition impose (downstream) technical challenges such as riboflavin, which

201   fluoresces, and folate, which is difficult to dissolve and likely to precipitate during media

202   preparation; (iii) removal of trace elements that are likely to precipitate; (iv) removal of all

203   non-essential nucleic acid precursors; (v) adjustment of phosphate concentration such that it

204   provides enough buffering capacity to enable growth until OD_{600} of 0.8, while not inhibiting

205   growth rate; (vi) adjustment of amino acid composition to 2.5-fold the requirement for 1

206   gDW·L^{-1} according to the biomass composition (Oliveira et al. 2005); and (vii)

207   implementation of a new protocol that reduces variations between media batches by avoiding

8

208 precipitation and heat or light degradation. Glucose was added to a final concentration of 25

209 mM and cultivation was performed under an anaerobic headspace.

210

211 ***Standardized cryopreservation and inoculation procedure***

212 The outcome of laboratory evolution experiments can be greatly affected by the composition

213 of the population used to seed each of the prolonged cultivations. In order to minimize

214 background genetic variation and variations in pre-culture condition, we developed a

215 standardized cryopreservation and inoculation procedure inspired by industrial procedures to

216 create, maintain and distribute single strain isolate stocks (Figure 1, main text). All the

217 prolonged cultivations in this study were carried out from the working stocks generated via

218 this procedure.

219 *Single colony isolation and parent-stock preparation*

220 A glycerol stock of *L. lactis* MG1363 (provided by Jan Kok, University of Groningen, the

221 Netherlands) was used to inoculate M17 enriched with 0.5% glucose (GM17). This culture

222 was streaked out from GM17 onto CDMPC agar plates (CDMPCA) and incubated for 48

223 hours at 30º C. An isolated colony was transferred to CDMPC and incubated for 24 hours at

224 30º C. A 1% inoculum of the freshly grown culture was used to inoculate CDMPC. After 5

225 consecutive transfers under the same conditions and using 1% inoculum to seed subsequent

226 cultures, the resulting culture was streaked out in CDMPCA and incubated for 24 hours at 30º

227 C. An isolated colony was transferred to 7.5 ml of CDMPC and incubated for 24 hours at 30º

228 C reaching a final OD_{600} of 1.165. "Parent-stocks" were then prepared by adding 3.75 ml of

229 sterile 60% glycerol and dividing the mixture in 11 aliquots of 1 ml in self-standing Nunc™

230 Cryotubes (366656), kept at -80º C for at least for 48 hours before reviving or moving.

231 *Working-stock preparation*

232 One of the 11 aliquots of the parent-stock was used to inoculate 199 ml of CDMPC (0.5%

233 inoculum) and incubated for 20 hours at 30º C, until the culture was full-grown. 100 ml of

234 sterile 60% glycerol was then added, resulting in 300 ml of 20% glycerol stock of *L. lactis*

235 G0 in CDMPC. "Working-stocks" were then prepared by dividing the latter in 960 aliquots of

236 0.3 ml in 1.2 ml sterile polypropylene cluster tubes 96-well racked from Corning

237 Incorporated Costar® (4413). These were capped using 8-Cap Strips from Corning

238 Incorporated Costar® (4418) and separated into individual vials using a slightly heated

239 bistoury and ruler. Working-stocks were stored at – 80º C for at least 24 hours before

240 reviving or moving.

241 *Standardized inoculation procedure*

242   A working-stock was revived by thawing a 0.3 ml aliquot of 20% glycerol stock of *L. lactis*

243   G0 in CDMPC and used to inoculate 44.7 ml of CDMPC (0.67% inoculum). This culture was

244   incubated for 16 hours at 30º C, which corresponds to the time at which the culture reaches

245   early stationary phase (OD_{600} ~1.00±0.15). This freshly-grown culture cultivated in a

246   standardized fashion and seeded from a controlled inoculum, was then used directly as the

247   inoculum of downstream cultivations and assays (chemostats, batch cultures, etc.) performed

248   by different experimentalists across several laboratories committed to working in a

249   standardized way.

250   *Moving and storage of cryopreserved stocks*

251   The 11 aliquots of 20% glycerol stock of *L. lactis* G0 in CDMPC (parent-stock) were divided

252   amongst the laboratories of the University of Amsterdam, VU University Amsterdam,

253   Groningen University and Research Center and Wageningen University, preserved in

254   different -80º C freezers within these institutes. The 960 aliquots of 20% glycerol stock of *L.*

255   *lactis* G0 in CDMPC (working-stock) were divided amongst all the collaborators involved in

256   standardized systems biology studies using *L. lactis* G0 as the model organism. Both the

257   parent- and working-stocks were kept frozen at all times and transported accordingly.

258

259   ***Experimental set up***

260   *L. lactis* MG1363 was cultivated in 4 chemostats run in parallel at 30°C at the following

261   dilution rates: 0.5 h^{-1} for a total of 309 consecutive generations; 0.6 h^{-1} for a total of 700

262   consecutive generations. Our design makes use of bioreactor lids that can fit any vessel with a

263   GL45 thread. It allows for two connectors to be inserted at variable depths, used here to

264   control the working volume and sampling. These custom made bioreactors were set-up to

265   make four parallel chemostat cultivations controlling stirring, temperature, pH, flow, volume

266   and gas composition. The newly developed caps are versatile and can be readily adapted to

267   other types of controlled cultivation, such as fed-batch, pH-auxostats, turbidostats,

268   retentostats, amongst others. Culture samples can be withdrawn directly through a port

269   present in the centre of the cultivation vessel or by rerouting the effluent using acetal quick-

270   disconnect couplings (Masterflex via Cole Parmer, Schiedam, Netherlands) Throughout the

271   prolonged cultivations samples were collected from the effluent to leave the cultivation

272   undisturbed.

273   For each set of parallel chemostats, temperature was controlled using a water bath (Thermo

274   Haake DC30-W13/B via Cole Parmer, Schiedam, Netherlands) set to 30ºC. Even stirring was

275 ensured using an immersible stirrer unit connected to a remote controller (Cole Parmer,
276 Schiedam, Netherlands) set to ~300 rpm. Mixing was tested by pulsing with glucose to a final
277 concentration of 60 mM and taking samples at three different positions of the bioreactor.
278 Minor differences were observed between samples harvested at different time points (<5%),
279 and at small-time scales (<10 seconds) the solution appeared equilibrated. pH was measured
280 separately in each culture using a 120 mm gel-filled pH-sensor (Applikon, Schiedam,
281 Netherlands) connected to an Alpha-pH800 (Eutech, Thermoscientific) that controlled a 1
282 rpm L/S pump drive equipped with an Easy-Load II pump head (Masterflex via Cole Parmer,
283 Schiedam, Netherlands) that titrated the culture with a solution of 2.5 M NaOH. The culture
284 was continuosly flushed through the headspace with a mixture of 5% CO_2 and 95% N_2 at a
285 flow rate of 10 culture volumes per hour (i.e. 600 ml/h). The dilution rates of the different
286 prolonged cultivations carried out in this study were set by controlling the flow of CDMPC
287 using a variable speed L/S pump drive equipped with four Easy-Load II pump heads
288 (Masterflex via Cole Parmer, Schiedam, Netherlands). All parallel cultivations were supplied
289 with CDMPC from the same medium vessel.
290 A small sample was removed every 10-15 generations and stored at -80 °C in 20% (v/v)
291 glycerol. In addition, the effluent was collected for optical density at 600 nm (OD_{600})
292 measurements and HPLC analysis. For subsequent studies, the glycerol stocks were used. 5
293 ml of fresh CDMPC was inoculated from the frozen glycerol stocks and grown for 16 h at
294 30°C. The overnight culture was subsequently diluted to a starting OD_{600} of 0.025-0.050 in
295 either CDMPC or M17 medium (Oxoid, Basingstoke, United Kingdom) supplemented with
296 0.5% (w/v) glucose or other carbon sources as indicated.

297 *Pyrosequencing*
298 Frozen glycerol stocks served as template material for PCR reactions. The PyroMark
299 platform from QIAGEN was used for pyrosequencing and reactions were performed as per
300 manufacturer's instructions. The region surrounding the point mutations was amplified and
301 biotinylated with the use of a biotinylated reverse primer. To detect the ratio of SNPs in the
302 population, single stranded primers were designed so as to terminate before the codon
303 containing the mutation.

304 *Recombinant DNA methods*
305 For cloning purposes, *Escherichia coli* XL1 blue was used. *ccpA* from the evolved *L. lactis*
306 strains was cloned into the pQE30 plasmid essentially as described to create pQE30ccpA
307 (Kowalczyk and Bardowski 2003). This allowed for the placement of 6 X His at the 5'-end of

11

308 the *ccpA* gene. The *ccpA* gene was PCR amplified from genomic DNA from the single
309 colony isolates from strains Genr0, 309C1, 309C2 and 309C4. *E. coli* XL1blue harbouring
310 pQE30ccpA was used for overproduction of CcpA by IPTG induction. CcpA was purified
311 using Ni-NTA resin (Qiagen, Germantown, MD, USA) as previously described (Kowalczyk
312 and Bardowski 2003). The protein concentration was determined with the DC Protein assay
313 kit (Bio-Rad, Hercules, CA, USA) using BSA as a standard.

314

315 *Protein identification by liquid chromatography-mass spectrometry*

316 The samples were separated by SDS-PAGE and stained with Bio-Safe Coomassie (Bio-Rad,
317 Hercules, CA, USA). In-gel tryptic digestion was followed by peptide extraction and LC-
318 MS/MS as described in detail in Drop *et al.,* 2011. The MS raw data was submitted to Mascot
319 (Version 2.1, Matrix Science, London, UK) and searched against the *L. lactis* MG1363
320 proteome. Protein identifications were based on at least 2 unique peptides identified by
321 MS/MS, each with a confidence of identification probability of at least 95%.

322

323 *Molecular dynamics simulations*

324 The free energy of mutating the protein was calculated while protein was bound to DNA and
325 free in solvent and the relative binding free energy of the mutated protein compared to the
326 wild type was obtained by subtracting the free energy of the former from the latter
327 (Supplementary Figure 9).

328 The free energy of mutating the protein was calculated using a topology with two side chains
329 at residue 19. The two side chains did not interact with each other and the mutation was done
330 in three steps. In the first step, the charges of the wild type methionine side chain were
331 uncoupled from rest of the system while the mutated side chain was completely non-
332 interacting. In the second step, the Lennard-Jones interactions of methionine side chain were
333 uncoupled while at the same time the Lennard-Jones interactions of the mutated side chain
334 were coupled to the side chain. In the third step, the charges of the mutated side chain were
335 coupled to the system while the methionine side chain was completely non-interacting. The
336 first and third steps were performed using 5 simulations with different lambda values while
337 the second step used 11 lambda values. Soft-core interactions were used in the second step
338 with soft-core parameter α set to 0.5. An error estimate is calculated from block averaging

12

339   each 1 ns of the simulations and using the standard deviation of the obtained values as the

340   error.

341   In the simulations, the protein monomers can move relatively freely in solution when DNA is

342   not present and sampling of conformations becomes an issue. To ensure that the

343   conformations sampled would be similar for all CcpA variants, rotational and translational

344   constraints were used to prevent the monomers from moving with reference to each other as

345   described in (50).

346   A 2 fs time step was used with all bonds constrained using the LINCS algorithm (Hess et al.

347   1997). Simulations were run with periodic boundary conditions in all directions. Non-bonded

348   interactions were treated as recommended in (Bjelkmar et al. 2010). Electrostatics were

349   calculated using PME (Essmann et al. 1995) with a 1.2 nm cut-off. Lennard-Jones

350   interactions were switched off between 1.0 and 1.2 nm and dispersion correction was applied

351   to both energy and pressure. The protein-DNA system and the solvent were separately

352   coupled to a 298 K heat bath using the velocity rescaling thermostat (Bussi et al. 2007) with

353    $\tau_T = 0.5$ ps. A 1 bar pressure was kept using an isotropic Parrinello-Rahman (Parrinello and

354   Rahman 1981) pressure coupling with $\tau_p = 4.0$ ps and 4.5e-5 bar^{-1} compressibility. Each

355   system was energy minimized and briefly equilibrated with position restraints before being

356   equilibrated for 10 ns. After equilibration each simulation was run for 20 ns except the

357   systems with deviant *cre* sites that were simulated for 10 ns.

358   All simulations were run using the Gromacs 4.5.5 (Hess et al. 2008) simulation package. The

359   protein and DNA were modelled with CHARMM27 force field with CMAP corrections

360   (Foloppe and MacKerell Jr. 2000; MacKerell et al. 2004) together with the original TIP3P

361   water model (Jorgensen et al. 1983) as implemented in Gromacs 4.5.5.

362   Free energy changes were calculated from simulations using the Bennett acceptance ratio

363   method (Bennett 1976) with the g_bar tool in Gromacs. Gromacs is a free software package

364   available at http://www.gromacs.org/.

365

366   ***Enzyme reactions***

367   L-lactate dehydrogenase (L-LDH) was purchased from Sigma-Aldrich (St. Louis, MO, USA).

368   L-LDH was added to culture supernatant to a final concentration of 0.2U/ml, NADH was

369   added to 2 mM and the reaction incubated for 15 minutes at 25°C. X-prolyl dipeptidyl

370   aminopeptidase (PepX) activity was measured using the chromogenic substrate Ala-Pro-*p*-

371   nitroanilid (Bachem Feinchemicalien AG, Bubendorf, Switzerland) as described (Buist et al.

372   1998).

373   β-galactosidase assays were performed as previously described (Israelsen et al. 1995;

374   Kloosterman et al. 2006).

375

376   ***Miscellaneous***

377   Oligopeptides were from JPT Peptide Technologies GmbH (Berlin, Germany).

378

379

380   **Supplementary References**

381   Ashkenazy H, Erez E, Martz E, Pupko T, Ben-Tal N. 2010. ConSurf 2010: calculating
382   evolutionary conservation in sequence and structure of proteins and nucleic acids.
383   Nucleic Acids Res. 38:W529–W533.

384   Bennett CH. 1976. Efficient estimation of free energy differences from Monte Carlo data. J.
385   Comput. Phys. 22:245–268.

386   Bjelkmar P, Larsson P, Cuendet MA, Hess B, Lindahl E. 2010. Implementation of the
387   CHARMM Force Field in GROMACS: Analysis of Protein Stability Effects from
388   Correction Maps, Virtual Interaction Sites, and Water Models. J. Chem. Theory
389   Comput. 6:459–466.

390   Brooijmans RJW, Poolman B, Schuurman-Wolters GK, de Vos WM, Hugenholtz J. 2007.
391   Generation of a membrane potential by *Lactococcus lactis* through aerobic electron
392   transport. J. Bacteriol. 189:5203–5209.

393   Buist G, Kok J, Eenhouts K, Dabrowska M, Venema G, Haandrikman AJ. 1995. Molecular
394   Cloning and Nucleotide Sequence of the Gene Encoding the Major Peptidoglycan
395   Hydrolase of *Lactococcus lactis*, a Muramidase Needed for Cell Separation. J Bacteriol
396   177:1554–1563.

397   Buist G, Venema G, Kok J. 1998. Autolysis of *Lactococcus lactis* Is Influenced by
398   Proteolysis. J. Bacteriol. 180:5947–5953.

399   Bussi G, Donadio D, Parrinello M. 2007. Canonical sampling through velocity rescaling. J.
400   Chem. Phys. 126:14101.

401   Cesselin D, Lamberet G, Duwat P, Sourice S, Vido K, Gaudu P, Loir YLE, Violet F, Cesselin
402   B, Le Loir Y, et al. 2001. Respiration Capacity of the Fermenting Bacterium
403   *Lactococcus lactis* and Its Positive Effects on Growth and Survival. J. Bacteriol.
404   183:4509–4516.

405   Deutscher J, Francke C, Postma PW. 2006. How phosphotransferase system-related protein
406   phosphorylation regulates carbohydrate metabolism in bacteria. Microbiol. Mol. Biol.
407   Rev. 70:939–1031.

408   van Dijk M, Wassenaar TA, Bonvin AMJJ. 2012. A Flexible, Grid-Enabled Web Portal for
409   GROMACS Molecular Dynamics Simulations. J. Chem. Theory Comput. 8:3463–3472.

410   Essmann U, Perera L, Berkowitz ML, Darden T, Lee H, Pedersen LG. 1995. A smooth
411   particle mesh Ewald method. J. Chem. Phys. 103:8577–8593.

412   Foloppe N, MacKerell Jr. AD. 2000. All-atom empirical force field for nucleic acids: I.
413   Parameter optimization based on small molecule and condensed phase macromolecular
414   target data. J. Comput. Chem. 21:86–104.

415   Hess B, Bekker H, Berendsen HJC, Fraaije JGEM. 1997. LINCS: A Linear Constraint Solver
416   for Molecular Simulations. J Comput Chem 18:1463–1472.

417   Hess B, Kutzner C, van der Spoel D, Lindahl E. 2008. GROMACS 4: Algorithms for Highly
418   Efficient, Load-Balanced, and Scalable Molecular Simulation. J. Chem. Theory Comput.
419   4:435–447.

420   Israelsen H, Madsen SM, Vrang A, Hansen EB, Johansen E. 1995. Cloning and partial
421   characterization of regulated promoters from *Lactococcus lactis* Tn917-lacZ integrants
422   with the new promoter probe vector, pAK80. Appl. Environ. Microbiol. 61:2540–2547.

423   Jensen PR, Hammer K. 1993. Minimal Requirements for Exponential Growth of *Lactococcus*

424   *lactis*. Appl. Environ. Microbiol. 59:4363–4366.

425   Jorgensen WL, Chandrasekhar J, Madura JD, Impey RW, Klein ML. 1983. Comparison of
426   simple potential functions for simulating liquid water. J. Chem. Phys. 79:926–935.

427   Kloosterman TG, Hendriksen WT, Bijlsma JJE, Bootsma HJ, van Hijum SAFT, Kok J,
428   Hermans PWM, Kuipers OP. 2006. Regulation of Glutamine and Glutamate Metabolism
429   by GlnR and GlnA in *Streptococcus pneumoniae*. J. Biol. Chem. 281:25097–25109.

430   Kowalczyk M, Bardowski J. 2003. Overproduction and purification of the CcpA protein from
431   *Lactococcus lactis*. Acta Biochim Pol. 50:455–459.

432   Kuipers OP, de Jong A, Baerends RJS, van Hijum SAFT, Zomer AL, Karsens HA, den
433   Hengst CD, Kramer NE, Buist G, Kok J. 2002. Transcriptome analysis and related
434   databases of *Lactococcus lactis*. Antonie Van Leeuwenhoek 82:113–122.

435   Levdikov VM, Blagova E, Joseph P, Sonenshein AL, Wilkinson AJ. 2006. The Structure of
436   CodY, a GTP- and Isoleucine-responsive Regulator of Stationary Phase and Virulence in
437   Gram-positive Bacteria. J. Biol. Chem. 281:11366–11373.

438   Loll B, Kowalczyk M, Alings C, Chieduch A, Bardowski J, Saenger W, Biesiadka J. 2007.
439   Structure of the transcription regulator CcpA from *Lactococcus lactis*. Acta Crystallogr.
440   Sect. D 63:431–436.

441   MacKerell AD, Feig M, Brooks CL. 2004. Improved Treatment of the Protein Backbone in
442   Empirical Force Fields. J. Am. Chem. Soc. 126:698–699.

443   Oliveira A, Nielsen J, Förster J. 2005. Modeling *Lactococcus lactis* using a genome-scale
444   flux model. BMC Microbiol. 15:1–15.

445   Parrinello M, Rahman A. 1981. Polymorphic transitions in single crystals: A new molecular
446   dynamics method. J. Appl. Phys. 52:7182–7190.

447   Poolman B, Konings WN. 1988. Relation of growth of *Streptococcus lactis* and
448   *Streptococcus cremoris* to amino acid transport. J Bacteriol 170:700–707.

449   Sanz Y, Lanfermeijer FC, Hellendoorn M, Kok J, Konings WN, Poolman B. 2004. Two
450   homologous oligopeptide binding protein genes (oppA) in *Lactococcus lactis* opp2
451   [corrected]. Int. J. Food Microbiol. 97:9–15.

452   Schumacher MA, Sprehe M, Bartholomae M, Hillen W, Brennan RG. 2011. Structures of
453   carbon catabolite protein A-(HPr-Ser46-P) bound to diverse catabolite response element
454   sites reveal the basis for high-affinity binding to degenerate DNA operators. Nucleic
455   Acids Res. 39:2931–2942.

456   Thomas TD, Ellwood DC, Longyear VM. 1979. Change from homo- to heterolactic
457   fermentation by *Streptococcus lactis* resulting from glucose limitation in anaerobic
458   chemostat cultures. J. Bacteriol. 138:109–117.

459   Tynkkynen S, Buist G, Kunji E, Kok J, Poolman B, Venema G, Haandrikman A. 1993.
460   Genetic and biochemical characterization of the oligopeptide transport system of
461   *Lactococcus lactis*. J. Bacteriol. 175:7523–7532.

462

463

464

465 **Supplementary Figures Legends**

466

467

468 **Supplementary Figure 1.** Strain characteristics during the evolution experiments at D of
469 0.5h-1 and of the resulting evolved strains. For each of the chemostats (labeled C1 to C4) the
470 cell counts (A) and organic acids (B) were measured. The values for lactate (red), formate
471 (dark blue), acetone (blue) and ethanol (light blue) are shown. The levels of pyruvate
472 increased in all the chemostats during the evolution experiment (C). The evolved strains were
473 revived in batch culture and the growth characteristics determined (D).

474

475

476

477 **Supplementary Figure 2**. Transcriptional fidelity in evolved strains is comparable to the
478 original ones. Strains were grown in CDMPC and harvested at the mid-exponential phase of
479 growth. Data are averages of three measurements with the error bars indicating the standard
480 deviation. Specific β-galactosidase activity was measured in the strains indicated using pPG6
481 (P. Gamba and J.W. Veening, unpublished data), which contains a premature stop codon at
482 Glu13.

483

484

485 **Supplementary Figure 3.** Altered gene expression in evolved strains is focused on transport
486 pathways. Genes were considered to be significantly changes with a Bayes p-value score of
487 less than 0.05 and a pfp value of less than 0.05. Genes found to change significantly in the
488 evolved strains were grouped into functional classes. The p-value is the summation of the
489 hypergeometrical distribution and p-values less than 0.05 were considered to be significant.
490 (a) Over-represented KEGG BRITE classes found. (b) Over-represented regulons found. (c)
491 The expression of genes involved in glucose uptake in *L. lactis* MG1363 were significantly
492 changed in the evolved strains. Highlighted in green are genes that were up-regulated and in
493 red for down-regulated. Gene expression changes not meeting the significance cut-off values
494 are highlighted in grey. (d) Kinetic parameters of glucose transport in Genr0 and the evolved
495 stains were determined in cells grown to exponential phase in CDMPC. Glucose transport
496 was assayed with the use of [14-C]-labeled glucose. Values of three independent
497 experiments were averaged and are reported ±SD. Vmax and Km were determined using
498 glucose concentrations from 1.2 to 200 μM.

499

500

Supplementary Figure 4. (a) Rate of utilization of carbon sources present in biolog plates. Cells were grown in CDMPC until mid-exponential phase, washed in CDMPC without glucose and resuspended in CDMPC without glucose containing 5 µg/mlchloramphenicol to an OD600 of 2. 150 µl of the culture suspension was added to each of the wells of the biology plate and acid formation was monitored at OD485 for 4 hours. The maximum rates of utilization were calculated and the averages of two separate experiments are shown. Only susbtrates used by at least one strains are shown. (b) Substrates not utilized under the conditions tested.

509

510

511 **Supplementary Figure 5.** Growth of the evolved strains is inhibited but not abolished when
512 leucine is supplied as a nonapeptide. (a) Differentially expressed genes involved in
513 oligopeptide uptake in *L. lactis* MG1363. Significant changes were considered for genes with
514 a Bayes p-value score ofless than 0.05 and a pfp value of less than 0.05 and are highlighted in
515 green for upregulated genes and in red for down regulated genes. Gene expression changes
516 not meeting the significance cut off values are highlighted in grey. (b) Strains were grown in
517 CDMPC or in CDMPC without leucine but with a leucine-containing nonapeptide.Growth
518 was followed for 16 hours. Shown are Gen0 (black lines) and 309F4 (grey lines) grown in
519 CDMPC (solid lines) or CDMPC with leucine-containing peptide (dashed lines). (c) The
520 difference in the final OD600 values reached after growth for 16 hours are shown for all
521 strains. Shown are the averages between three separate experiments with the standard
522 deviation indicated.

523

524

525   **Supplementary Figure 6.** Evolved strains are less prone to lysis on prolonged cultivation
526   than the original strain. (a) Expression changes for acmA are shown. Differentially expressed
527   genes involved in aerobic respiration in L. lactis MG1363. Significant changes were
528   considered for genes with a Bayes p-value score ofless than 0.05 and a pfp value of less than
529   0.05 and are highlighted in red for down regulated genes. (b) PepX activity was measured in
530   the culture supernatant at the time points indicated. Activity was measured using the
531   chromogenic substrate Ala-Pro-p-nitroanilid and the colour change was monitored at OD405.
532   One representative experiment is shown. (c) Evolved strains sediment during growth.
533   Overnight cultures of Gen0 and 309C1 in CDMPC are shown. (d) Sedimentation is caused
534   by the formation of long cell chains. Typical pictures are shown for Gen0 and 309C1 grown
535   for 16 hours in CDMPC. The cells were visualized using a Zeiss light microscope and a Zeiss
536   digital camera. Magnification, ×1 000.

537

538

539   **Supplementary Figure 7.** Evolved cells are no longer able to respire when heme is added to
540   the medium. (a) No biomass increase is observed in the evolved strains when heme is added
541   to the growth medium. Strains were grown in GM17 medium for 16 hours under aerobic
542   conditions with and without heme which was added to 2 μg/ml. Shown are the average
543   values from three separate experiments with the standard deviation indicated. (b)
544   Differentially expressed genes involved in aerobic respiration in *L. lactis* MG1363.
545   Significant changes were considered for genes with a Bayes p-value score of less than 0.05
546   and a pfp value of less than 0.05 and are highlighted in red for down regulated genes. Gene
547   expression changes not meeting the significance cut off values are highlighted in grey.

548

549

550 **Supplementary Figure 8.** The DNA binding domain of CcpA is highly conserved. (a)
551 Using consurf db (Ashkenazy et al. 2010) and the *B. subtilis* CcpA-HPr complex bound to a
552 synthetic cre site (3OQN) as a starting structure, the level of amino acid sequence
553 conservation among LacI transcriptional regulators was analysed. One molecule of CcpA is
554 colored according to the level of conservation within the LacI family of transcriptional
555 regulators, HPr and the DNA are colored yellow. Dark purple indicates 100% conservation
556 while blue indicates extensive sequence variation. (b) View of the DNA-binding domain
557 with the side chain of Met19 (numbering according to *L. lactis* MG1363) is shown.

558

559

560   **Supplementary Figure 9.** The thermodynamic cycle to calculate the relative binding free
561   energies. The wild type protein is shown in yellow and the mutated protein in red. Note that
562   while the color of the whole protein is different only a single residue is changed in both
563   monomers of the mutated protein. The relative binding free energy is $\Delta G1 + \Delta G3$ which,
564   based on the cycle, is equal to $-(\Delta G2 + \Delta G4)$. The inset highlights the DNA binding domain
565   of CcpA, with the methionine-19 position in red, and isoleucine at the same position in
566   yellow.

567

568 **Supplementary Figure 10.** Binding of CcpA to cre sites in vitro. The binding of CcpA-
569 Met19 and CppA-Ile19 was tested with DNA sequences identified as cre sites upstream of
570 *ptcB* and *mtlD* as well as a perfect cre site referred to as syn. As a control the CodY
571 recognition site upstream of *oppD* was also tested.

572

573

574

575 **Supplementary Figure 11.** *ccpA* accumulates the Met19 to Ile early in evolution experiment
576 and quickly takes over the population. The abundance of the three CcpA species is shown.
577 Indicated are the averages of two pyrosequencing reactions and in the case of strain 309C4,
578 the abundance of the Thr mutation was verified by Sanger sequencing.   The PCR was
579 performed from the frozen stocks sampled during the continuous culture process. In green is
580 indicated the prevalence of the Ile mutant, in blue wild type CcpA and in grey the Thr
581 mutant. (a) 309C1, (b) 309C2, (c) 309C3, (d) 309C4.

582

583

584 **Supplementary Figure 12.** Abundance of nucleotides at third position in the Met19 codon.
585 Indicated are the averages of two pyrosequencing reactions. The PCR was performed from
586 the frozen stocks sampled during the continuous culture process. In green is indicated the
587 prevalence of adenosine, in red thymine, in blue cytosine and in black guanine. The average
588 standard deviation between the separate reactions was 4.4. (a) 309C1, (b) 309C2, (c) 309C3,
589 (d) 309C4.

590

591

592   **Supplementary Figure 13. Overview of the fitting results.** A & B. The fitted model (eq. 2
593   and 3) and the experimental data. C. Predicted dynamics of the concentration of the limiting
594   nutrient in the chemostat. The mutant wins the competition with the wild type because it can
595   grow at a specific growth rate equal to D at a lower limiting nutrient concentration than the
596   wild type. D. Influence of parameter values on the objective, indicating that all the parameter
597   values reach their optimal values (reported in Supplementary Table 1) when the fit objective
598   reaches its minimal value. E. Illustration that the Monod constant of the wild type and the
599   mutant cannot be independently estimated; i.e. the same objective value is obtained for
600   different values of those parameters. The plot suggests that the ratio of Kw/Km can be fitted
601   but not their individual values.

602
603
604
605
606
607
608
609
610
611

a KEGG BRITE — hypergeometrical distribution ($e^{-p\text{-value}}$)

- amino acid transporter, AAT family
- arginine:ornithine antiporter/ lysine permease
- carbohydrate metabolism
- amino acid metabolism
- membrane transport

b REGULON — hypergeometrical distribution ($e^{-p\text{-value}}$)

- ArgR
- CodY
- HrcA
- AhrC
- CcpA
- PyrR

c fold change in expression level

ptcB *ptcA* *llmg_0439* — PTS^{Cel} low affinity Km = 8.7 mM

ptnD *ptnC* *ptnAB* — PTS^{Man} high affinity Km = 13 µM

glcU — Glucose permease Km = 2.4 mM

d

Strain	Glucose uptake and metabolism	
	Vmax (nmol/min x mg protein)	Km (µM)
Genr0	176.0 ± 13.1	21.0 ± 0.8
309C1	484.7 ± 37.2	22.2 ± 0.7
309C2	488.9 ± 45.4	21.5 ± 1.2
309C3	507.9 ± 48.3	21.8 ± 1.7
309C4	419.6 ± 49.4	21.4 ± 1.6

a
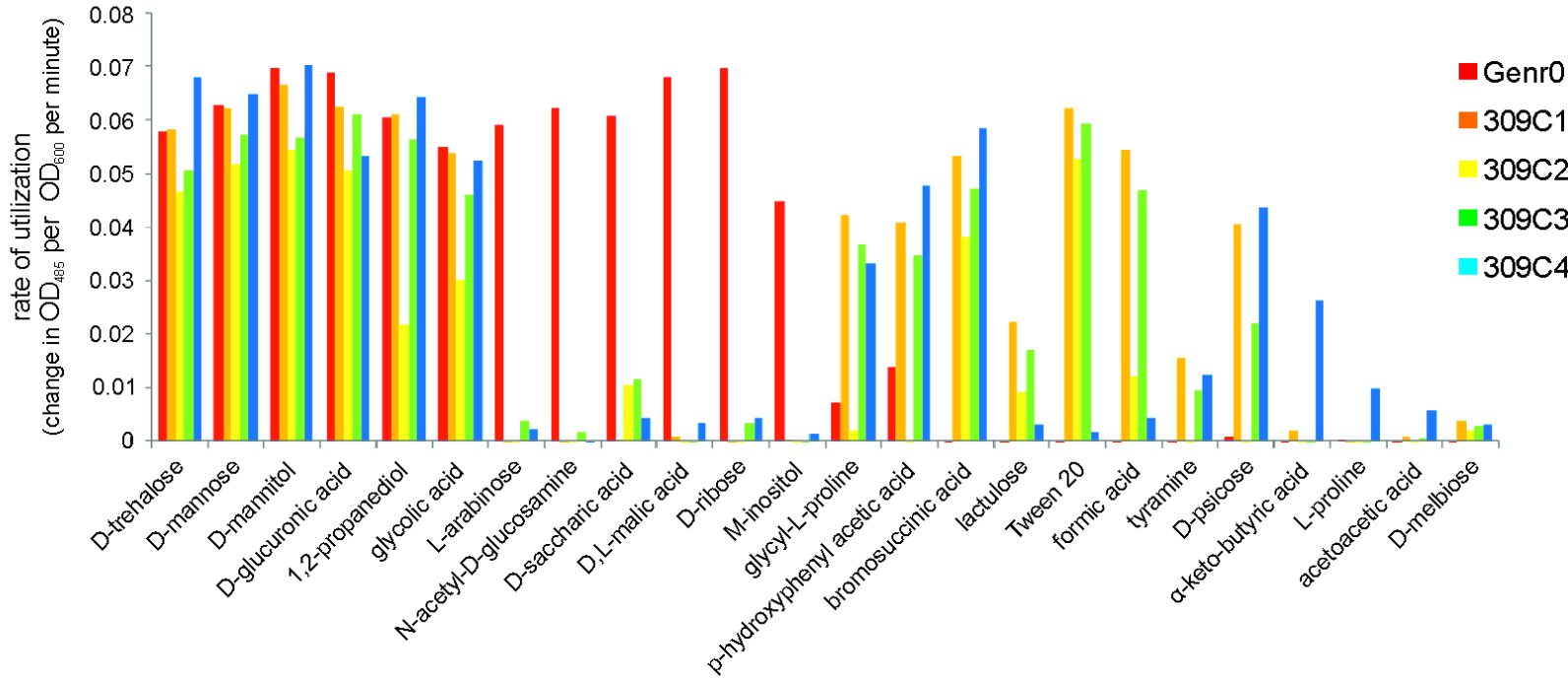
b

2-aminoethanol	β-methyl-D-glucoside	D-glucosaminic acid	glycyl-L-aspartic acid	L-lactic acid	mucic acid
2-deoxy adenosine	citric acid	D-glucose-1-phosphate	glycyl-L-glutamic acid	L-malic acid	N-acetyl-β-D-mannosamine
acetic acid	D,L-α-glycerol-phosphate	D-glucose-6-phosphate	glyoxylic acid	L-proline	phenylethylamine
acetoacetic acid	D-alanine	D-malic acid	inosine	L-serine	propionic acid
adenosine	D-aspartic acid	D-serine	L-alanine	L-threonine	pyruvic acid
adonitol	D-cellubiose	D-sorbitol	L-alanyl-glycine	L-xylose	succinic acid
α-D-glucose	D-fructose	D-threonine	L-asparagine	maltose	sucrose
α-D-lactose	D-fructose-6-phosphate	Dulcitol	L-aspartic acid	maltotriose	thymidine
α-hydroxy butyric acid	D-galactonic acid-γ-lactone	D-xylose	L-fucose	methyl pyruvate	tricarballylic acid
α-hydroxy glutaric acid-γ-lactone	D-galactose	fumaric acid	L-galatonic acid-γ-lactone	m-hydroxy phenyl acetic acid	Tween 40
α-keto-glutaric acid	D-galaturonic acid	glucuronamide	L-glutamic acid	mono methyl succinate	Tween 80
α-methyl-D-galactosidase	D-gluconic acid	glycerol	L-glutamine	M-tartaric acid	uridine

a

	309C1	309C2	309C3	309C4
oppA	-2.51	-1.77	-6.78	-8.47
oppB	-2.07	-1.55	-4.28	-6.55
oppC	-2.81	-1.89	-6.62	-8.29
oppD	-1.93	-1.84	-4.48	-9.83
oppF	-2.10	-1.79	-6.51	-6.93
oppA2	-1.75	1.18	-1.68	4.13
oppB2	-1.35	1.55	-1.12	5.53
oppC2	1.08	2.05	1.06	2.28

b

SLSQSKVLP
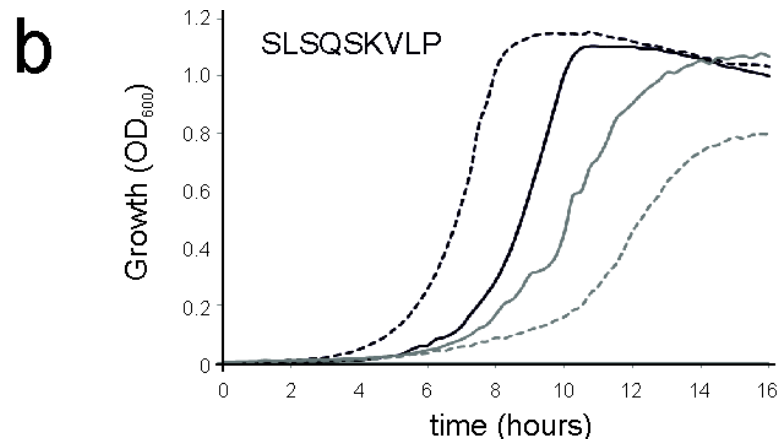
c

Strain	Difference in maximum OD$_{600}$ reached with oligopeptide (%)
Genr0	103.4 ± 1.65
309C1	75.08 ± 6.68
309C2	103.2 ± 12.49
309C3	77.72 ± 0.08
309C4	74.18 ± 3.85
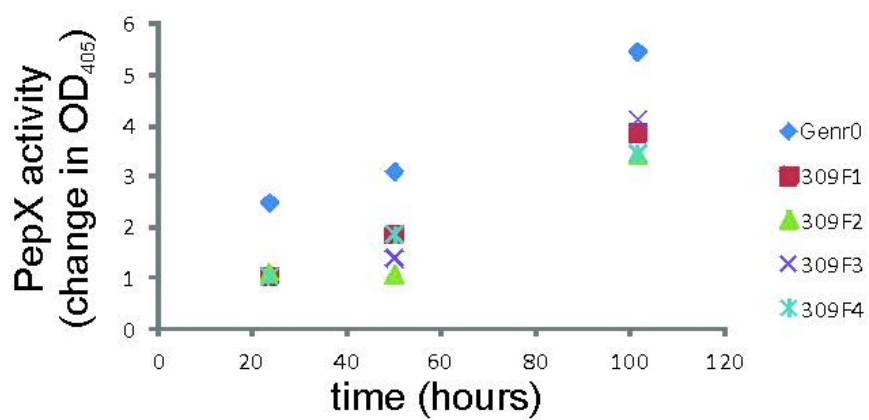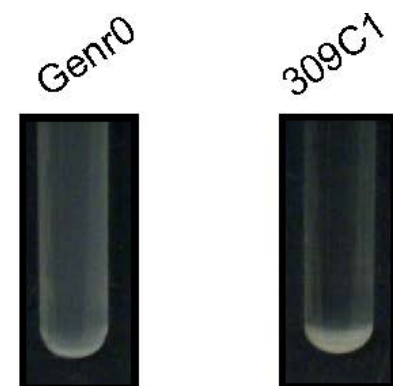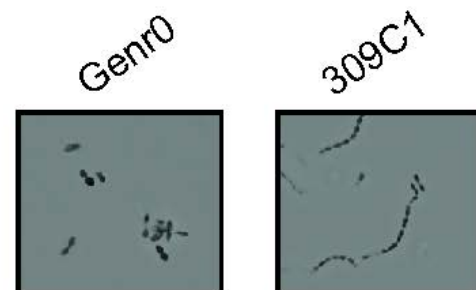
a

strain	GM17	GM17 + heme	ratio
Genr0	2.48 ± 0.005	4.22 ± 0.16	1.70
309F1	2.13 ± 0.04	2.32 ± 0.025	1.09
309F2	2.24 ± 0.015	2.42 ± 0.02	1.08
309F3	2.49 ± 0.03	2.68 ± 0.025	1.08
309F4	2.08 ± 0.005	2.38 ± 0.005	1.14

b

	309C1	309C2	309C3	309C4
noxA	1.00	-1.14	-1.72	-2.05
noxB	-1.82	-1.53	-1.02	-2.18
noxE	-2.44	-1.93	-2.99	-1.30
hemK	-1.72	-1.86	-2.02	-1.22

variable — conserved

Promoter sequence   *syn*   *ptcB1*   *mtlD*   *oppD*

CcpA-Met[19]

CcpA-Ile[19]